

The cyst-theca relationship of the dinoflagellate cyst *Trinovantedinium pallidifulum*, with erection of *Protoperidinium louisianensis* sp nov and their phylogenetic position within the Conica group

Mertens Kenneth ^{1,11,*}, Gu Haifeng ², Takano Yoshihito ³, Price Andrea M. ⁴, Pospelova Vera ⁵,
Bogus Kara ⁶, Versteegh Gerard J. M. ^{7,12}, Marret Fabienne ⁸, Turner R. Eugene ⁹,
Rabalais Nancy N. ¹⁰, Matsuoka Kazumi ³

¹ Univ Ghent, Res Unit Palaeontol, Krijgslaan 281 S8, B-9000 Ghent, Belgium.

² SOA, Inst Oceanog 3, Xiamen 361005, Peoples R China.

³ Inst East China Sea Res EC SER, 1551-7 Taira Machi, Nagasaki 8512213, Japan.

⁴ McGill Univ, Dept Geog, Burnside Hall, 805 Sherbrooke St West, Montreal, PQ H3A OB9, Canada.

⁵ Univ Victoria, Sch Earth & Ocean Sci, OEASB A405, POB 1700 STN CSC, Victoria, BC V8W 2Y2, Canada.

⁶ Texas A&M Univ, Int Ocean Discovery Program, 1000 Discovery Dr, College Stn, TX 77845 USA.

⁷ MARUM Ctr Marine Environm Sci, Leobener Str, D-28359 Bremen, Germany.

⁸ Univ Liverpool, Sch Environm Sci, Liverpool L69 7ZT, Merseyside, England.

⁹ Louisiana State Univ, Dept Oceanog & Coastal Sci, Baton Rouge, LA 70803 USA.

¹⁰ Louisiana Univ Marine Consortium, Chauvin, LA 70344 USA.

¹¹ IFREMER, LER BO, Stn Biol Marine, PI Croix, BP40537, F-29185 Concarneau, France.

¹² Helmholtz Zentrum Polar & Meeresforsch, AWI, Handelshafen 12, D-27570 Bremerhaven, Germany.

Corresponding author : Kenneth Mertens, email address : kenneth.mertens@ifremer.fr

Abstract :

We establish the cyst-theca relationship of the dinoflagellate cyst species *Trinovantedinium pallidifulum* Matsuoka 1987 Matsuoka K. 1987. Organic-walled dinoflagellate cysts from surface sediments of Akkeshi Bay and Lake Saroma, North Japan. Bulletin Faculty of Liberal Arts, Nagasaki University (Natural Science) 28:35–20. [Google Scholar] based on germination experiments of specimens isolated from the Gulf of Mexico. We show that the motile stage is a new species, designated as *Protoperidinium louisianensis*. We also determine its phylogenetic position based on single-cell polymerase chain reaction (PCR) of a single cell germinated from the Gulf of Mexico cysts. To further refine the phylogeny, we determined the large subunit (LSU) sequence through single-cell PCR of the cyst *Selenopemphix undulata* isolated from Brentwood Bay (Saanich Inlet, BC, Canada). The phylogeny shows that *P. louisianensis* is closest to *P. shanghaiense*, the motile stage of *T. applanatum*, and is consistent with the monophyly of the genus *Trinovantedinium*. *Selenopemphix undulata* belongs to a different clade than *Selenopemphix quanta* (alleged cyst of *P. conicum*), suggesting that the genus *Selenopemphix* is polyphyletic. *Trinovantedinium pallidifulum* is widely distributed with occurrences in

the Gulf of Mexico, the North Atlantic, the northeast Pacific and southeast Asia. In addition, we illustrate the two other extant species, *Trinovantedinium applanatum* and *Trinovantedinium variabile*, and two morphotypes of *Trinovantedinium*. Geochemical analyses of the cyst wall of *T. pallidifulum* indicate the presence of amide groups in agreement with other heterotrophic dinoflagellate species, although the cyst wall of *T. pallidifulum* also includes some unique features.

Keywords : Micro-FTIR, *Selenopemphix undulata*, Wadden Sea, Lake Saroma, Saanich Inlet, Gulf of Mexico

1. Introduction

The heterotrophic thecate dinoflagellate genus *Protoperidinium* Bergh is characterized by possessing three cingular plates and an additional transitional plate (Balech 1974). This large genus currently encompasses approximately 280 species (Gómez 2012). The identification of the thecate stage of *Protoperidinium* species is based on the body size, outline, presence and position of apical and/or antapical horns/spines, cingulum displacement and particularly the plate pattern (e.g., Hoppenrath et al. 2009). In regard to the thecal plate arrangement, Balech (1974) used the number of anterior intercalary plates and precingular plates to subdivide *Protoperidinium* into three subgenera: the subgenus *Protoperidinium*, which has seven precingular plates and three anterior intercalary plates; the subgenus *Minusculum*, which has six precingular plates and three anterior intercalary plates; and the subgenus *Archaeperidinium*, which has seven precingular plates and two anterior intercalary plates. Later, the subgenus *Testeria* was erected by Faust (2006) to accommodate species with seven precingular plates, one anterior intercalary plate and no apical pore complex. However, the results from molecular phylogeny questioned the validity of the subgenus *Minusculum* because it was nested within the subgenus *Protoperidinium* (Yamaguchi et al. 2007; Ribeiro et al. 2010), and showed the polyphyly of the subgenus *Archaeperidinium*, as originally described by Jørgensen (1912) (Ribeiro et al. 2010). *Archaeperidinium* was, therefore, emended as a genus and characterized by the flat sulcus, sulcal flagellar fin covering the sulcal area and circular cingulum without displacement (Yamaguchi et al. 2011).

The subgenus *Protoperidinium* can be subdivided into several sections based on the shape of the first apical (1') plate (ortho, meta or para) and the shape of the second anterior intercalary (2a) plate (quadra, penta or hexa) (e.g., Gribble and Anderson 2006). Molecular phylogenies suggested that most of these sections are monophyletic and nested within the *Protoperidinium* sensu stricto clade (Mertens et al. 2013; Gu et al. 2015). There are only two exceptions: the section *Conica* is polyphyletic and positioned within the *Protoperidinium* sensu stricto clade (Yamaguchi et al. 2006; Gu et al. 2015), and the section *Oceanica* is monophyletic but positioned outside of the *Protoperidinium* sensu stricto clade (Sarai et al. 2013).

Several *Protoperidinium* species have been associated ~~with~~ a particular cyst, and the morphology of these cysts can be taxonomically informative, especially the shape of ~~the opening in the cyst wall, termed~~ the archeopyle (Harland 1982). Thecate stages belonging to *Protoperidinium* and *Archaeperidinium* with a transitional plate ~~have cysts~~ generally ~~have~~with a saphopylic or theroptylic 2a archeopyle ~~of their respective cyst~~ (Harland 1982; Ribeiro et al. 2010; Mertens et al. 2012a) whereas, *Protoperidinium* species without a transitional plate have ~~cysts with~~ a compound archeopyle involving 2'-4' (Lewis & Dodge 1987; Kawami & Matsuoka 2009; Kawami et al. 2009; Mertens et al. 2013; Liu et al. 2014). Cyst morphology can be diverse and is used to classify cysts into various cyst-~~defined~~ genera such as *Brigantedinium* Reid, *Votadinium* Reid and *Selenopemphix* Benedek (Fensome et al. 1993). However, differences between the cyst-~~based-defined~~ nomenclature and the motile-~~based-defined~~ nomenclature have not yet been fully reconciled.

1
2
3
4
5
6
7
8
9
10
11
12
13
14
15
16
17
18
19
20
21
22
23
24
25
26
27
28
29
30
31
32
33
34
35
36
37
38
39
40
41
42
43
44
45
46
47
48
49
50
51
52
53
54
55
56
57
58
59
60

Trinovantedinium Reid is a cyst-based-defined genus erected by Reid (1977) to describe peridiniacean cysts with an intercalary archeopyle because, at that time, the existence of such an archeopyle in the genus *Lejeunecysta* Artzner & Dörhöfer 1978 was in doubt. This initial diagnosis included species with or without processes on the cyst. The genus was subsequently emended by Harland (1977), Bujak (1984) and de Verteuil & Norris (1992). The latter restricted the diagnosis of *Trinovantedinium* to only include biphragmal cysts with short, penitabular and intratabular, but never sutural, hollow to solid processes. There are currently 11 species within this genus (Table 1). The type species was described by Reid (1977) and is the large transparent *Trinovantedinium capitatum* from recent-modern Rosslare Point sediment (Ireland). Later, this was considered a junior synonym of *Lejeunia applanata*, described by Bradford (1977) from recent sediments off the east coast of the Musandam Peninsula (Oman), which was renamed later as *Trinovantedinium applanatum* (for details see de Verteuil & Norris 1992, p. 408). This is the first of only three species from this genus that are considered extant; the other eight species are extinct (Table 1). *Trinovantedinium pallidifulum* is the second extant species, first described by Matsuoka (1987) from Holocene surface sediments in Akkeshi Bay (Hokkaido, Japan). The third is *Trinovantedinium variabile*, described by Bujak (1984) from the early Pliocene of the Bering Sea, and was recorded as extant by Radi & de Vernal (2004), Pospelova et al. (2008), Krepakevich & Pospelova (2010), Price & Pospelova (2011) and Bringué et al. (2013).

For only one of these extant species is the cyst-theca relationship and molecular phylogenetic position known. The cyst-theca relationship for the type species *Trinovantedinium applanatum* was first established by Wall & Dale (1968); however, it was mistakenly related to *Protoperidinium pentagonum* (Gran) Balech. This error was propagated in subsequent studies (Matsuoka 1982; Lewis et al. 1984; Baldwin 1987). It was Inoue, H. in Fukuyo et al. (1990, p. 154–155) who first remarked that the cingulum of the *T. applanatum* thecate stage has no displacement, in contrast with *P. pentagonum*. Gu et al. (2015) re-established the cyst-theca relationship for *T. applanatum* from the East China Sea, and they erected the species *Protoperidinium shanghaiense* to describe the motile stage. The hexa-ortho configuration placed this species in the *Conica* group and its LSU rDNA sequence was closest to *P. divaricatum*, *P. leonis* and *P. conicum*. This cyst-theca relationship was most recently confirmed by Li et al. (2015).

In this study, we establish the cyst-theca relationship for the second extant species of the genus *Trinovantedinium*, *T. pallidifulum*, through incubation of surface sediments from the Gulf of Mexico, Dee Estuary (United Kingdom), and Wadden Sea (Germany). We erect a new species, *Protoperidinium louisianensis*, to describe the motile stage of *Trinovantedinium pallidifulum*. We obtained LSU rDNA sequences through single-cell PCR that show the motile stage is closest to *Protoperidinium shanghaiense*. In addition, we document the distribution of *Trinovantedinium pallidifulum* and the geochemical composition of its cyst wall. We also illustrate the two other extant species, *Trinovantedinium applanatum* and *Trinovantedinium variabile*. Finally, to further constrain the phylogeny, we also resolve the phylogenetic position of *Selenopemphix undulata* from Brentwood Bay (B.C., Canada).

2. Material and methods

2.1. Germination experiments

We collected cysts of *Trinovantedinium pallidifulum* for incubation studies from surface sediment samples at three locations: (1) northern Gulf of Mexico, (2) Dee Estuary (UK), and (3) the Wadden Sea in northern Germany (Figure 1 and Table 2). All samples were stored in plastic

1
2
3
4
5
6
7
8
9 135 bags and refrigerated at 4 °C. In situ sea-surface salinities (SSSs) and sea-surface temperatures
10 136 (SSTs) were measured when collecting the samples (Table 2).

11 137 Approximately 0.5–1.0 cm³ of wet sediment was immersed in filtered seawater after
12 138 which it was ultrasonicated in a bath (60 s) and rinsed through a 20 µm nylon mesh using filtered
13 139 seawater. The cyst fraction was separated from this residue using heavy liquid sodium
14 140 polytungstate (density = 1.3 g cm⁻³) (Bolch 1997). Single cysts were then transferred to Nunclon
15 141 0.5 ml microwells subjected to an irradiance of 100 µmol photons m⁻² s⁻¹ and 24 h light, and
16 142 filled with L1 medium. The wells were kept at room temperature. Cysts were regularly checked
17 143 for germination, and observations were performed under an Leitz DM inverted light microscope.
18 144 Encysted and excysted cysts as well as motile cells were photographed and measured using an
19 145 Leica DM 5000B light microscope equipped with a Leica DFC 490 camera with 100x oil
20 146 immersion objectives. For each motile cell, the length, width, depth, distance between the tips of
21 147 the antapical horns, and width of the cingulum were measured, as where possible. For each cyst,
22 148 the same parameters were measured; additionally, the length of three randomly chosen spines per
23 149 cyst were measured. All measurements in the species descriptions cite, in order: the minimum,
24 150 average (in parentheses) and maximum values (in µm). The standard deviation (SD) is also
25 151 provided where appropriate. Incubation experiments were done by KNM and took place at
26 152 GEOTOP (Gulf of Mexico and Dee Estuary samples) and Univ. of Bremen (Wadden Sea
27 153 samples). All measurements were done by KNM.

28 154 We also attempted to germinate *Selenopemphix undulata* from Saanich Inlet (Canada),
29 155 but none of the isolated cysts germinated.

30 156 2.2. Study of cysts from surface sediments

31 157 To determine the distribution of *Trinovantedinium pallidifulum*, permanent slides of surface
32 158 samples were examined which included locations from the the northeastern and northwestern
33 159 Pacific and the northern Gulf of Mexico (Figure 1 and Table 2). Routine palynological
34 160 techniques were used for processing (Pospelova et al. 2004; Matsuoka et al. 2003; Mertens et al.
35 161 2012b). The samples were oven-dried at 40 °C and then treated with room-temperature 10%
36 162 hydrochloric acid (HCl) to remove calcium carbonate. The material was rinsed twice with
37 163 distilled water, sieved at 120 µm to eliminate the coarse fraction, and retained on a 15 µm nylon
38 164 mesh. To dissolve siliceous particles, samples were treated with 48–50% room-temperature
39 165 hydrofluoric acid (HF) for at least two days, and then treated for 10 min with room-temperature
40 166 HCl (10%) to remove fluorosilicates. The residue was rinsed twice with distilled water,
41 167 ultrasonicated for 30 s and finally collected on a 15 µm mesh. Residue aliquots were mounted in
42 168 glycerine jelly. All measurements and light photomicrographs were as described in Section 2.1.
43 169 In addition, in order to illustrate *Trinovantedinium applanatum* and *Trinovantedinium variabile*,
44 170 we re-examined permanent slides from palynologically prepared samples from several localities.
45 171

46 172 2.3. Single-cell PCR amplification and sequencing of the motile stage of

47 173 *Trinovantedinium pallidifulum*

48 174 Surface sediment samples containing *Trinovantedinium pallidifulum* were used from the Gulf of
49 175 Mexico (Figure 1 and Table 2). Cysts were isolated from the sediment using the heavy liquid
50 176 separation described in Section 2.1. Motile cells identified through light microscopy were rinsed
51 177 several times in sterilized distilled water, broken by compressing the cell between the slide and
52 178 cover slip, and then transferred into a PCR tube. The single cell was used as the template to
53 179 amplify about 1200 bp of the nuclear-encoded LSU rDNA, using the primers D1R (Scholin et al.
54 180

1
2
3
4
5
6
7
8
9
10
11
12
13
14
15
16
17
18
19
20
21
22
23
24
25
26
27
28
29
30
31
32
33
34
35
36
37
38
39
40
41
42
43
44
45
46
47
48
49
50
51
52
53
54
55
56
57
58
59
60

1994) and 28-1483R (Daugbjerg et al. 2000). A 50 µl PCR cocktail containing 0.2 µM primers, PCR buffer, 50 µM dNTP mixture, 1U of Ex Taq DNA polymerase (Takara, Dalian, China) was subjected to 35 cycles using a Mastercycler PCR (Eppendorf, Hamburg, Germany). The PCR protocol was: initial denaturation for 3.5 min at 94 °C, followed by 35 cycles of 50 s denaturation at 94 °C, 50 s annealing at 45 °C, and 80 s extension at 72 °C, plus a final extension of 10 min at 72 °C. The amplified products were run on a 1% agarose gel. Positive bands were excised and purified using a DNA extraction kit (Sangon, Shanghai, China) and sequenced in both directions using the ABI Big-Dye dye-terminator technique (Applied Biosystems, Foster City, California, USA), according to the manufacturer recommendations. [This DNA work was performed by HG in Third Oceanographic Centre, Xiamen, China.](#)

2.4. *Single-cell PCR amplification and sequencing of cysts of *Selenopemphix undulata**

We obtained surface sediment samples containing *Selenopemphix undulata* from Brentwood Bay (B.C., Canada) (48,58°N,-123.47°E, 6 m water depth) using a petite ponar grab on October 1, 2011. Cysts were isolated from the sediment using heavy liquid separation as described in Section 2.1. The cysts were then rinsed several times in sterilized distilled water, broken by compressing the cell between the slide and cover slip, and then transferred into a PCR tube. The single cell was used as the template to amplify about 1200 bp of the nuclear-encoded LSU rDNA, using the primers D1R (Scholin et al. 1994) and 28-1483R (Daugbjerg et al. 2000). A 50 µl PCR cocktail containing 0.2 µM primers, PCR buffer, 50 µM dNTP mixture, 1U of Ex Taq DNA polymerase (Takara, Dalian, China) was subjected to 35 cycles using a Mastercycler PCR (Eppendorf, Hamburg, Germany). The PCR protocol was an initial denaturation for 3.5 min at 94 °C, followed by 35 cycles of 50 s denaturation at 94 °C, 50 s annealing at 45 °C, and 80 s extension at 72 °C, plus a final extension of 10 min at 72 °C. The amplified products were run on a 1% agarose gel. Positive bands were excised and purified using a DNA extraction kit (Sangon, Shanghai, China) and sequenced in both directions using the ABI Big-Dye dye-terminator technique (Applied Biosystems, Foster City, California, USA), according to the manufacturer's recommendations. [This DNA work was performed by YT at the University of Nagasaki, Japan.](#)

2.5. *Sequence alignments and phylogenetic analyses*

Newly obtained sequences were first aligned with those of related species available in GenBank using 'BioEdit' v7.0.0 (Hall 1999), and subsequently using Mafft (Katoh et al. 2005) (<http://mafft.cbrc.jp/alignment/server/>). *Akashiwo sanguinea* (Hirasaka) G. Hansen & Moestrup was selected as the outgroup. A Bayesian reconstruction of the data matrix was performed with MrBayes 3.0b4 (Ronquist & Huelsenbeck 2003) using a general time reversible model (GTR +I+G) chosen by JmodelTest (Posada 2008). Four Markov chain Monte Carlo (MCMC) chains ran for two million generations, sampling every 1,000 generations with a burnin of 10%. A majority rule consensus tree was created in order to examine the posterior probabilities of each clade. Maximum likelihood-based analyses were conducted with RaxML v7.2.6 (Stamatakis 2006) on the T-REX web server (Boc et al. 2012) using the above model. Bootstrap values were determined with 1,000 replicates.

2.6. *Geochemical analysis of cyst wall chemistry*

After germination, an empty cyst originally derived from surface sediment of the Wadden Sea (Germany) (Figure 1) was removed from a microwell using a micropipette into a droplet of water contained on a glass slide with a concave depression. The water was allowed to evaporate and

then a droplet of ethanol was added. The cyst was allowed to soak in the ethanol for 30 min after which a droplet of MilliQ water was added. The cyst was then isolated and the procedure repeated twice. These steps were to ensure that any polar or apolar compounds adhered to the cyst wall were removed. The cyst was then visually examined under the light microscope and placed on an Au-coated mirror and analysed with micro-Fourier transform infrared spectroscopy using a Bruker FT-IR microscope (Hyperion 3000) with a 15x objective. The spectrum was acquired in reflective mode with 50 scans over 4000-600 cm⁻¹ and is shown after background subtraction. Peak assignments were based on Colthup (1990) and relevant published literature (e.g., Bogus et al. 2012; 2014; Cárdenas et al. 2004; Versteegh et al. 2012). [This geochemical work was done by KB, KNM and GJMV at the Univ. of Bremen, Germany.](#)

3. Results

3.1. Results of germination experiments

Undescribed motile cells, here assigned to *Protoperidinium louisianensis* n. sp., emerged from *Trinovantedinium pallidifulum* cysts isolated from surface sediments of the Gulf of Mexico (five specimens identified) (Figure 1 and Table 1). [These motile cells germinated from the cysts](#) After one or two days of incubation, ~~motile cells germinated from the cysts~~. These cells died a few days after germination and never divided. Two out of four specimens of *Trinovantedinium pallidifulum* from the Wadden Sea (Germany) germinated, but the cells did not fully develop thecal plates. A single specimen from [the](#) Dee Estuary (UK) germinated, but the motile stage could not be fully observed.

3.2. Systematic palaeontology

Division DINOFLAGELLATA (Bütschli 1885) ~~emend.~~ Fensome et al. 1993, emend. Adl et al. 2005

Class DINOPHYCEAE Pascher 1914

Subclass PERIDINIPHYCIDAEE Fensome et al. 1993

Order PERIDINIALES Haeckel 1894

Family PROTOPERIDINIACEAE Balech 1988 nom. cons.

Subfamily PROTOPERIDINIOIDEAE (Autonym)

Genus *Protoperidinium* Bergh 1881

Protoperidinium louisianensis Mertens, Gu, Price et Matsuoka n. sp.

Plate 1, figures 1–15, Plate 2, figures 1-15

Holotype. Plate 1, figures 1–9.

Type locality. Northern Gulf of Mexico, station A7 (28.94°N, 89.75°W), offshore Louisiana.

Diagnosis. A species of intermediate size of the genus *Protoperidinium* with the tabulation formula Po, X, 4', 3a, 7'', 3c+t, ?s, 5''', 2'''''. The motile cell is pentagonal in outline and dorsoventrally flattened, with a short apical horn and two antapical horns, each bearing a short spine. The epitheca is longer than the hypotheca, and bears convex sides. Plate 1' is ortho-type, 1a and 3a are penta-type, and 2a is hexa-type and stenodeltaform linteloid. Plates are thin with polygonal reticulations. The cyst is pentagonal and light brown in color, with a thickened apical horn and two thickened antapical horns. The cyst surface is smooth, bearing numerous peritabular, short, solid, erect, and non-branching processes with acuminate tips. Sometimes the dorsal side of the hypotheca is striated. The archeopyle is stenodeltaform linteloid, angular and saphopylic.

1
2
3
4
5
6
7
8
9
10
11
12
13
14
15
16
17
18
19
20
21
22
23
24
25
26
27
28
29
30
31
32
33
34
35
36
37
38
39
40
41
42
43
44
45
46
47
48
49
50
51
52
53
54
55
56
57
58
59
60

272 | **Derivation of name.** The specific epithet refers to the type locality, which liesis offshore the
273 | state of Louisiana (USA).

274 | **Gene sequence.** The LSU rDNA gene sequence of the cyst—GenBank Accession No.

275 | KU519754XXXXXX (LSU).

276 | **Description.** *Description of motile cell of* *Protoperidinium louisianensis* (Plate 1, figures 1–9,
277 | Plate 2, figures 1–9). The excysted motile cells (five observed and not preserved) were
278 | pentagonal in outline, dorsoventrally flattened and carried an apical horn and two antapical horns
279 | of equal length, each bearing a short spine (Plate 1, figure 1–2, Plate 2, figure 1). The epitheca
280 | had convex sides and was longer than the hypotheca. The cell contents were greenish, except for
281 | a red body. The thin thecal plates carried polygonal reticulations (Plate 1, figure 2,7).

282 | The plate arrangement on the epitheca was bilaterally symmetrical. The oval apical pore
283 | plate (Po) was surrounded by a low apical collar formed by the raised edges of the apical plates
284 | (Plate 2, figure 4). The canal plate (X) was elongate and trapezoidal (Plate 2, figure 4). The first
285 | apical plate (1') was wide and rhombic (ortho-type) and the sides of plate 1' contacting plates 2'
286 | and 4' are longer than those contacting plates 1'' and 7'' (Plate 1, figure 2). Plates 2' and 4' were
287 | elongated and subpentagonal, whereas 3' was short and subpentagonal (Plate 1, figure 4). The
288 | first and third anterior intercalary plates (1a) were pentagonal and equal in size (Plate 1, figures
289 | 3,6). The second anterior intercalary plate (2a) was hexagonal, stenodeltaform linteloid and more
290 | elongated and had two small sides touching plates 3'' and 5'' (Plate 1, figure 4). The precingular
291 | series consisted of seven plates. Plate 1'', 4'' and 7'' were quadrangular (Plate 1, figures 2,4), and
292 | 2'', 3'', 5'' and 6'' pentagonal (Plate 1, figures 3,5,6). The cingulum was slightly left-handed
293 | (descending), lined with narrow lists and comprising three cingular plates plus a transitional
294 | plate. The transitional plate (t) was small. Plate 1c reached the end of plate 1'' and 2''' (Plate 1,
295 | figure 3). Plate 2c was the longest of the series and reached a short way beyond the 6''/7''
296 | boundary and the 4'''/5''' boundary (Plate 1, figure 7). Plate 3c was similar in size to Plate 1c.

297 | We were unable to dissect and observe all the sulcal plates.

298 | The plate arrangement of the hypotheca was also symmetrical, featuring five postcingular
299 | plates. Plate 5''' was longer than plate 1'''. Plates 1''', 3''', and 5''' were pentagonal, and 2''' and
300 | 4''' were quadrangular (Plate 1, figures 7–9). The antapical series comprised two plates, 1'''' and
301 | 2'''', which formed the antapical horns (Plate 1, figure 7).

302 | The plate formula is thus Po, X, 4', 3a, 7'', 3c+t, ?s, 5''', 2''''', and the complete tabulation
303 | (except for the sulcal plates) is illustrated in Figure 2.

304 | *Description of cyst of* *Protoperidinium louisianensis* (Plate 1, figures 10–15, Plate 2, figures 10–
305 | 15). Cysts were similar in shape to the motile stage, but light brown in color, bearing numerous
306 | small solid spines. The cysts were peridinioid (pentagonal) with a thickened apical horn and two
307 | thickened antapical horns of equal length. Living cysts contained abundant greenish granules.

308 | The epicyst had convex sides and was always longer than the hypocyst. The central body wall
309 | was thin (>0.3 µm) and biphragmal with closely appressed layers that separate along the apical
310 | horn and antapical horns, with a smooth surface (Plate 1, figure 11). Sometimes striations were
311 | present on the dorsal side of the hypocyst (Plate 2, figure 15). The processes were short, solid,
312 | erect, and non-branching with acuminate tips (Plate 1, figure 11). The process distribution was
313 | largely peritabular-penitabular (Plate 1, figure 13, Plate 2, figure 11). The process length was
314 | fairly constant for individual specimens, except around the apical horn and antapical horns where
315 | they became longer (Plate 2, figure 10). The paracingulum was excavated with lists ornamented
316 | with rows of equidistant processes, and slight left-handed displacement (Plate 2, figure 11). The
317 | parasulcus was free of processes and indented (Plate 1, figure 14), two flagellar scars were

Formatted: Font: Times New Roman, 12 pt

1
2
3
4
5
6
7
8
9 318 always visible (Plate 2, figure 12). The archeopyle was angular and saphopylic, involving release
10 319 of plate 2a, steno-deltaform linteloid. The description is based on cysts used in the incubation
11 320 experiments and those recovered from sediment and prepared using palynological methods.
12 321 Cysts without cell content in the palynologically treated samples did not retain their shape well -
13 322 they did not seem to be very robust as they were always quite folded and flattened.

14 323 **Dimensions.** Incubated motile cells: length, 52.3 (58.8) 65.1 μm (SD = 6.0, n=4); width, 44.0
15 324 (53.6) 58.8 μm (SD = 7.4, n=4); depth, 34.8 (38.4) 41.9 μm (SD = 5.0, n=2); distance between
16 325 the tips of the antapical horns, 12.8 (16.3) 20.3 μm (SD = 3.7, n=4); width of cingulum, 3.9 (4.1)
17 326 4.4 μm (SD = 0.2, n=4).

18 327 Cysts germinated to give identifiable thecae: length, 43.0 (58.5) 68.4 μm (SD = 8.2, n=10);
19 328 width, 46.3 (56.5) 63.9 μm (SD = 5.0, n=10); depth, 30.4 (40.6) 48.4 μm (SD = 7.2, n=7);
20 329 distance between the tips of the antapical horns, 16.0 (23.9) 27.7 μm (SD = 3.6, n=10); width of
21 330 cingulum, 4.5 (6.0) 7.2 μm (SD = 0.8, n=10); average length of three spines per cyst, 1.1 (1.8)
22 331 2.7 μm (SD = 0.4, n=30).

23 332 Cysts palynologically prepared from surface sediments of different locations: length, 49.9 (56.6)
24 333 62.8 μm (SD = 5.7, n=5); width, 49.8 (56.3) 63.3 μm (SD = 5.0, n=5); depth, none measured;
25 334 distance between the tips of the antapical horns, 20.6 (21.3) 22.5 μm (SD = 0.8, n=5); width of
26 335 cingulum, 4.8 (5.6) 6.5 μm (SD = 0.7, n=4); average length of three spines per cyst, 1.4 (1.9) 2.8
27 336 μm (SD = 0.4, n=15).

28 337 **Comments.** The geological preservability of the cysts was demonstrated by their ability to
29 338 withstand palynological treatment and presence in sediments at least as old as Holocene
30 339 (Matsuoka et al. 1999) to mid-Miocene (our interpretation of the "undefined proteroperidiniacean
31 340 species" depicted in de Verteuil & Norris (1992), plate 2, figs. 9–12). Specimens from the
32 341 German Wadden Sea show an identical morphology (Plate 3, figures 1–12) and the cysts
33 342 correspond to the cyst-~~based-defined species~~*taxon* *Trinovantedinium pallidifulum* Matsuoka,
34 343 here reillustrated by its holotype (Plate 3, figures 13–16).

34 344
35 345 | Genus *Trinovantedinium* Reid 1977, emend. de Verteuil & Norris 1992

36 346 | *Tinovantedinium applanatum* (Bradford 1977) Bujak & Davies 1983

37 347 | Plate 4, figures 1–13, Plate 5, figures 1–10

38 348 **Synonyms.** *Trinovantedinium capitatum* Reid 1977, Plate 1, figures 6–8.

39 349 **Comments.** The illustrated specimens conform to the original description of Bradford (1977).
40 350 We also illustrate two extreme morphotypes of this species. Type A (Plate 5, figures 1–7) was
41 351 found in warmer water regions (Omura Bay, Japan; Bay of Bengal; Red Sea) and shows a more
42 352 elongate, transparent body shape with straight sides and more elongated horns, separated by a
43 353 deep depression. Type B (Plate 5, figures 8–10) was found in cold water (offshore Greenland)
44 354 and shows a more rounded, transparent body shape with reduced horns and a very shallow
45 355 depression between the antapical horns. *Trinovantedinium applanatum* differs from
46 356 *Trinovantedinium pallidifulum* in its transparency, often larger and more elongate body and
47 357 longer processes.

48 358 | *Trinovantedinium variabile* (Bujak 1984) de Verteuil & Norris 1992

49 359 | Plate 6, figures 1–11

50 360 **Comments.** The illustrated specimens conform to the original description of Bujak (1984). The
51 361 holotype is redescribed and reillustrated by Head (1994, p. 226, pl. 11, figs. 4.5, 7.8).
52 362
53
54
55
56
57
58
59
60

Formatted: French (France)

Genus *Selenopemphix* Benedek 1972, emend. Head 1993

Selenopemphix undulata Verleye, Pospelova, Mertens et Louwye 2011, [Plate 1, figure 8](#)
Plate 6, figures 12–14

Comments. One cyst corresponding to *Selenopemphix undulata* as described by Verleye et al. (2011, [particularly the specimen displayed in Plate 1, figure 8](#)) was isolated for single-cyst PCR (Plate 6, figures 12–14). The cyst was collected from surface sediment of Brentwood Bay (B.C., Canada). The cyst was large and polar compressed, with a cingulum with [undulating](#)-margins [showing very small undulations](#). The epicyst was conical and striated, the hypocyst was also striated and bore two fused antapical horns that were wider than the apical horn. The archeopyle could not be observed on encysted specimens. The single cyst had a length of 44.5 μm (apex to antapex), width of 74.6 μm , and depth of 70.8 μm .

Gene sequence. [The LSU rDNA gene sequence of the cyst—GenBank Accession No. LC114019 \(LSU\).](#)

3.3. *Phylogenetic position of Protoperidinium louisianensis and Selenopemphix undulata as inferred from LSU rDNA sequences*

We obtained 1,143 base pairs from one germinated cell of *Protoperidinium louisianensis* isolated from the Gulf of Mexico (Accession number: [KU519754XXXXXX](#)), and this sequence was used for the phylogenetic analyses (Figure 3). *Protoperidinium louisianensis* was closest to *Protoperidinium shanghaiense*, and formed a clade with several other species belonging to the *Conica* section (*P. divaricatum*, *P. conicum*, *P. leonis*). *Selenopemphix undulata* ([Accession number: LC114019](#)), was closest to *Protoperidinium biconicum*, which also belongs to the section *Conica* and formed a separate clade with *P. punctulatum* and *P. humile*, both species belonging to the section *Tabulata*. The other members of the Protoperidiniaceae formed several other clades, which were also used by Gu et al. (2015).

3.4. *Modern Recent distribution of Trinovantedinium pallidifulum and inferred ecology*

Trinovantedinium pallidifulum was initially described by Matsuoka (1987) from Akkeshi Bay (Hokkaido, Japan) and subsequently predominantly in southeast Asia, [such as including](#) surface sediments off South Korea (Cho et al. 2003; Shin et al. 2011), Japan (Kojima et al., 1994; Matsuoka et al. 2003), China (Wang et al. 2004), and Malaysia (Furio et al. 2006) (Figure 1)).

In this study we show that this species is much more widely distributed since it is recorded in surface sediments from the northern Gulf of Mexico, Casino Coast (Brazil), the North Atlantic (La Vilaine Bay, Wadden Sea (Germany), Dee Estuary (UK), Kattegat), NW Pacific (Tokyo Bay and Ariake Sound, both in Japan) and the NE Pacific (Vancouver Island, Canada) (Table 2 and Figure 1). We also identify a specimen from the German Bight depicted by Nehring (1997, his figures 23–24, as *Trinovantedinium capitatum*) also as *T. pallidifulum*. The highest relative abundance of *T. pallidifulum* [eysts](#) was recorded in a surface sample from the Gulf of Mexico where [itthe eysts](#) contributes up to 3.8% of the cyst assemblages (Table 2). *T. pallidifulum* was found in this study in surface sediment samples corresponding to SSTs of ~ 11.30 – 31.45 $^{\circ}\text{C}$ and SSSs with a range of 8.60–33.61 psu (Table 2).

3.5. *Trinovantedinium pallidifulum* cyst wall chemistry

The spectrum produced by micro-FTIR analysis of the cyst wall (Figure 4) shows: a broad peak centered at 3340 cm^{-1} (OH stretching), weak peaks at 2920 and 2860 cm^{-1} (aliphatic CH stretching), peaks at 1780 and 1700 cm^{-1} (C=O stretching), 1630 cm^{-1} (C=C, C=O stretching)

Formatted: Font: Times New Roman, 12 pt

410 (amide I), 1585 and 1560 cm^{-1} (CN stretching, NH bending (amide II)), 1440 and 1405 cm^{-1}
 411 (CH bending), 1350 cm^{-1} (NO_2 , CCH_3 (not indicated in Figure 4)), 1310 cm^{-1} (amide III), 1255
 412 cm^{-1} (NH bending), 1140 and 1030 cm^{-1} (C-O stretching), and 890, 850 and 770 cm^{-1} (CH out of
 413 plane).

414

415 4. Discussion

416 4.1. Comparative morphology of the motile stage of *P. louisianensis* within the *Conica* 417 group

418 The motile stage of *P. louisianensis* can be distinguished from all species from the *Conica* group
 419 by the unique combination of excavated antapical horns each bearing a single spine, an epitheca
 420 with convex sides being longer than the hypotheca, a slightly left-handed cingulum, a
 421 stenodeltaform linteloid 2a and plates with polygonal reticulations. A few species show strong
 422 similarities. *P. conicum* also has spines on the antapical horns, but has an epitheca that is as long
 423 as the hypotheca, straight sutures from the apex of the cingulum and a more elongated pore (Gu
 424 et al. 2015). *P. shanghaiense* has no displacement of the cingulum, an epitheca with straight
 425 sides, two relatively closer antapical horns that bear no spines and a 2a that was isodeltaform
 426 linteloid (Gu et al. 2015). *P. conicoides* also bears spines on the antapical horns, but is more
 427 polar compressed. It also has an epitheca that is as long as the hypotheca, a 1''' which has a
 428 "nose" at the onset of the sulcus, and straight sutures from the apex to the cingulum (Hoppenrath
 429 et al. 2009, p. 158). The plates of *P. obtusum* and *P. leonis* are ornamented with longitudinal ribs
 430 (Hoppenrath et al. 2009, p. 158–159).

431

432 4.2. Comparative morphology of the cyst of *P. louisianensis* within the *Conica* group

433 The cyst of *P. louisianensis*, which corresponds to the cyst-based-defined species taxon
 434 *Trinovantedinium pallidifulum*, can be easily differentiated from all other species belonging to
 435 the genus *Trinovantedinium* (Table 1). The species differs from *Trinovantedinium applanatum*
 436 and *Trinovantedinium henrietii* because these are transparent and have an epicyst the same
 437 length as the hypocyst (Matsuoka 1987, Louwye et al. 2008). *Trinovantedinium boreale* is also
 438 transparent and has processes with platforms (Bujak 1984; see also Head 1994).
 439 *Trinovantedinium glorianum* has much more densely distributed and hollow processes and
 440 antapical horns that are sharper (Head et al. 1989). *T. variabile*, *T. harpagonium*, *T.*
 441 *ferruginomatium* and *T. sterthense* are more polar compressed with rounded antapical horns and
 442 bear longer processes with distal platforms or taeniate or aculeate processes (Bujak 1984, de
 443 Versteil & Norris 1992, Head 1993). *Trinovantedinium papula* and *Trinovantedinium?*
 444 *xylochoporum* are much more rounded and have longer processes (de Versteil & Norris 1992).

445

446 4.3. Validity of the ~~genus-genera~~ *Trinovantedinium* and *Selenopemphix*

447 The molecular phylogeny shows that *P. louisianensis* and *P. shanghaiense* are most closely
 448 related, which is thus the case for their respective cysts, *Trinovantedinium pallidifulum* and
 449 *Trinovantedinium applanatum*. This supports-is consistent with the monophyly of the genus
 450 *Trinovantedinium*. Whether this will be supported by the molecular characterization of the other
 451 extant species, *Trinovantedinium variabile*, should be the subject of further study.

452 The phylogenetic position of *Selenopemphix undulata* is more problematic because it is
 453 positioned in another clade than *Protoperidinium conicum*, the motile stage associated with the
 454 cyst-based taxon *Selenopemphix quanta* (note that this cyst-theca relationship needs further
 455 study, e.g. Matsuoka & Head 2013). This polyphyly suggests that both species belong to two

Formatted: Font: Not Italic

1
2
3
4
5
6
7
8
9
10
11
12
13
14
15
16
17
18
19
20
21
22
23
24
25
26
27
28
29
30
31
32
33
34
35
36
37
38
39
40
41
42
43
44
45
46
47
48
49
50
51
52
53
54
55
56
57
58
59
60

different genera, and their relatively long genetic distance suggests that they diverged a long time ago. This polyphyly is also supported by significant morphological differences between species of both cyst types, particularly the position of the archeopyle, which is more offset in *Selenopemphix undulata* (Verleye et al. 2009) than *Selenopemphix quanta* (it is considered central or slightly offset, see Head 1993, p. 31-32). It is, therefore, likely that *Selenopemphix quanta* should be transferred back to its initial name, *Multispinula quanta*. However, we suggest that the molecular phylogenetic position of the type species of *Selenopemphix*, *Selenopemphix nephroides*, the cyst considered to belong to *Protopteridinium subinerme* (Rochon et al. 1999) needs to be established before such a transfer. Either way, this result emphasizes the importance of the archeopyle position in cyst taxonomy, whereas the reniform cyst shape of both species, seems to be polyphyletic.

4.4. Validity of the genus Protopteridinium

Since long there has been a mismatch between paleontological and biological names, whereas several biological species that belong to the genus *Protopteridinium* have been associated with cysts belonging to different cyst-defined genera (e.g. *Brigantedinium*, *Quinquecuspis*, *Selenopemphix*, etc.) (e.g. Fensome et al. 1993). Although there have been attempts to reconcile both nomenclatural systems (e.g. Harland 1982), no consensus has yet been reached as how to resolve this issue and here we also suggest to respect the status quo in order to avoid further confusion.

Formatted: Font: Bold

4.4.4.5. Evolution of *Trinovantedinium* and *Selenopemphix* within the *Peridinales*

Previous studies have tried to elucidate evolutionary patterns based on the morphologic changes of the motile stages (e.g., Taylor 1980) or on the basis of cyst morphology (e.g., Bujak & Davies 1983). Molecular phylogenetics largely support the biological approach which focuses on variations in tabulation, and consider the *Monovela* group and *Diplopsaloideans* as ancestral to the *Protopteridinium sensu stricto* group (e.g., Liu et al. 2015a,b; Gu et al. 2015; Mertens et al. 2015). Both of these ancestral groups have not been identified in the earlier fossil record of the *Peridinales* (Cretaceous – Eocene), and the cyst morphologies observed during this time period (Bujak & Davies 1983) are more similar to the cyst-based genera *Lejeunecysta*, *Quinquecuspis* and *Trinovantedinium*, which, based on molecular phylogenetics, belong to the *Protopteridinium sensu stricto* group (Figure 3). A reinvestigation of the fossil record is urgently needed to explain this discrepancy between the fossil record and the molecular phylogenetics, and begs the question whether preservation issues or the complex cyst identification of these relatively unknown ancestral species could be responsible, or if multigene phylogenies would also support the LSU based phylogeny (e.g., Orr et al. 2012).

Formatted: Bullets and Numbering

Trinovantedinium boreale would presumably be the oldest *Trinovantedinium* species, as it has been observed in the late Paleocene, since all other species have Miocene or later first ~~occurrences~~ appearances (Table 1). Two other closely related species to *Trinovantedinium applanatum* and *Trinovantedinium pallidifulum*, the cyst of *Protopteridinium divaricatum* (cyst-~~defined-based~~ name *Xandarodinium xanthum*) and the cyst of *Protopteridinium leonis* (cyst-~~defined-based~~ name *Quinquecuspis concreta*) (Figure 3) both have younger first ~~occurrences~~ appearances (Miocene ~~(Matsuoka, 1992);~~ and Pleistocene ~~(de Vernal et al., 1992);~~ respectively). Interestingly, the here documented *Trinovantedinium applanatum* type B shows similarities to *Trinovantedinium boreale*, although the latter has longer and fewer processes. It

Formatted: Font: Not Italic

1
2
3
4
5
6
7
8
9
10
11
12
13
14
15
16
17
18
19
20
21
22
23
24
25
26
27
28
29
30
31
32
33
34
35
36
37
38
39
40
41
42
43
44
45
46
47
48
49
50
51
52
53
54
55
56
57
58
59
60

would, therefore, be important to obtain a sequence from this type B and see how it relates to the other sequences.

4.5.4.6. Distribution of *Trinovantedinium pallidifulum*

T. pallidifulum was shown in this study to be widely distributed in temperate to tropical waters (Figure 1), in surface sediment samples corresponding to SSTs of ~11.30–31.45 °C and SSSs with a range of 8.60–33.61 psu.

4.6.4.7. Cyst wall geochemistry of *Trinovantedinium pallidifulum*

The *T. pallidifulum* cyst wall chemistry demonstrates a composition both consistent and dissimilar with other known heterotrophic dinoflagellates (Figure 4). The greatest similarity is the evidence for nitrogen-containing functional groups in the cyst wall, which is consistent with all previously analyzed cysts from heterotrophic dinoflagellates (Bogus et al. 2014). This evidence includes several absorptions indicative of amide groups (1630, 1585, 1560, 1310, and 1255 cm⁻¹). The presence of nitrogen-containing functional groups was suggested to reflect the heterotrophy of the dinoflagellate producing the cyst (Bogus et al. 2014), with the incorporation of prey waste products (high in nitrogen groups from the breakdown of proteinaceous material) into the cyst wall. Additionally, similar to other species, there is clear evidence for alcohol groups (3340, 1140 and 1030 cm⁻¹), although the strongest series of absorptions in *T. pallidifulum* is different. In fact, the most obvious difference in the cyst wall chemistry of *T. pallidifulum* compared to other heterotrophic dinoflagellates is the lack of the dominant series of absorptions characteristic for polysaccharides (Bogus et al. 2014; Versteegh et al. 2012). However, absorptions at 1140 and 1030 cm⁻¹ are present, indicating that sugars may still be present as part of the cyst wall. The strongest absorptions are at 890 and 850 cm⁻¹, which usually result from ring vibrations and is supported somewhat by the absorption at 1630 cm⁻¹. There is also evidence that this species has a cyst wall that contains a significant carboxylic acid/ester component (1780, 1700 cm⁻¹), which may increase the stability of the cyst wall polymer (Yang et al. 1996). This pattern has been suggested in some species of the fossil *Apectodinium* genus (Bogus et al. 2012). However, the cyst wall is not aliphatic because absorptions indicating aliphatic C-H stretching are weak, which is consistent with many dinoflagellate cysts (de Leeuw et al. 2004; Bogus et al. 2014; Versteegh et al. 2012). Therefore, the spectrum of *T. pallidifulum* is unique to any previously analyzed species because it appears to incorporate amide groups, similar to other heterotrophic species, and contain a higher abundance of ester groups, found only in two other fossil species thus far. These results suggest that dinoflagellate cyst wall chemistry may be more diverse than previously considered and further study is required.

5. Conclusions

- We document the cyst-theca relationship for the cyst-based taxon *Trinovantedinium pallidifulum*, and erect the species *Protoperidinium lousianensis* to describe the motile stage.
- LSU rDNA based phylogenies show the closeness of *P. lousianensis* and *P. shanghaiense*, and also of their respective cysts, *Trinovantedinium pallidifulum* and *Trinovantedinium applanatum*.
- The genus *Trinovantedinium* is monophyletic, whilst the genus *Selenopemphix* is polyphyletic.

Formatted: Font: Bold

Formatted: Bullets and Numbering

Formatted: Font: Bold

Formatted: Bullets and Numbering

Formatted: Font: Not Bold

- 1
2
3
4
5
6
7
8
9 546 • *Trinovantedinium pallidifulum* is widely distributed, and can be found at SSTs of
10 547 ~11.30–31.45 °C and SSSs of 8.60–33.61 psu.
11 548 • *Trinovantedinium pallidifulum*'s cyst wall chemistry is unique but contains amide
12 549 groups, which is consistent with other heterotrophic species.
13 550

14 551 Acknowledgements

15 552 Kenneth Neil Mertens is a postdoctoral researcher of FWO Belgium. Martin J. Head is
16 553 acknowledged for advice on the genus *Trinovantedinium*. Anna Godhe is thanked for providing a
17 554 sample from the Kattegat. Evelyne Goubert is thanked for providing a sample from La Vilaine
18 555 Bay and Jean-Pierre Debenay for samples from the Vie River estuary. We acknowledge the
19 556 Scripps Institution of Oceanography (SIO) Geological Collections and in particular Alex
20 557 Hangsterfer for sediment samples from the Bay of Bengal. Pieter R. Gurdebeke is thanked for
21 558 providing a nice specimen of *Trinovantedinium variabile*. K.N.M. and A.M.P. thank Anne de
22 559 Vernal for letting us use the equipment to conduct germination experiments at GEOTOP. Sofia
23 560 Ribeiro is thanked for loan of slides from Portugal. G.J.M.V. acknowledges support by the
24 561 German Science Foundation (Heisenberg fellowship VE486/2). A.M.P. acknowledges the
25 562 support of the Natural Science and Engineering Research Council of Canada (NSERC). Support
26 563 for ship time for Gulf of Mexico specimens was provided by the National Oceanic and
27 564 Atmospheric Administration, Center for Sponsored Coastal Ocean Research, under awards
28 565 NA06OP0528 and NA09NOS4780204 to Louisiana Universities Marine Consortium and awards
29 566 NA06OP0529 and NA09NOS4780230 to Louisiana State University. The crew of the R/V
30 567 *Pelican* is thanked for assistance with sample collection. [Martin J. Head and an anonymous](#)
31 568 [reviewer are thanked for remarks that significantly improved the manuscript.](#)

32 569 Author biographies

33 570
34 571
35 572 Kenneth Neil Mertens is a [postdoctoral-permanent](#) researcher at [Ghent University,](#)
36 573 [Belgium](#)[Ifremer, LER BO, Concarneau, France.](#) He received his Ph.D. in 2009 from Ghent
37 574 University. His research interests are the taxonomy, evolution, phylogeny and biogeography of
38 575 dinoflagellates, and the palaeoceanographical application of dinoflagellate cysts, particularly in
39 576 the Quaternary and Neogene.
40 577

41 578 Haifeng Gu is a Professor at Third Institute of Oceanography, China. He received his Ph.D. in
42 579 2007 from Ocean University of China. His research interests are taxonomy and evolution of
43 580 dinoflagellates.
44 581

45 582 Yoshihito Takano is a postdoctoral researcher at National Research Institute of Fisheries
46 583 Science, Fisheries Research Agency, Yokohama, Japan. He received his Ph.D. in 2006 from
47 584 Hokkaido University. His research interests are taxonomy and evolution of dinoflagellates.
48 585

49 586 Andrea Price is a PhD candidate in the Department of Geography at McGill University. She
50 587 recieved her BSc Honours and MSc in Earth and Ocean Sciences at the University of Victoria.
51 588 Her main research interests include using dinoflagellate cysts as indicators of water quality in
52 589 North American estuaries, the seasonality of cyst production, and the use of cysts in Quaternary
53 590 paleoceanographic studies.
54 591
55
56
57
58
59
60

1
2
3
4
5
6
7
8
9 592 | ~~Dr.~~ Vera Pospelova is an Associate Professor at the School of Earth and Ocean Sciences (SEOS),
10 593 | University of Victoria. She received her Honours BSc in Geology from ~~the~~ Novosibirsk
11 594 | University (Russia) and PhD in Physical Geography from McGill University (Canada). Vera's
12 595 | research interests include: taxonomy of late Quaternary dinoflagellate cysts; cyst production,
13 596 | ecology, and seasonal dynamics in coastal waters; applications of dinoflagellate cysts as
14 597 | indicators of water quality conditions, with the emphasis on pollution and eutrophication in
15 598 | North American estuaries, as well as paleoceanographic reconstructions using sedimentary
16 599 | archives.
17 600

18 601 | Kara Bogus is a staff scientist with the International Ocean Discovery Program (IODP) at Texas
19 602 | A&M University (College Station, TX, USA). She earned her PhD (marine geosciences) from
20 603 | the University of Bremen (Bremen, Germany). Her research interests include using organic-
21 604 | walled dinoflagellate cysts in paleoceanographic studies, cyst wall chemical composition and its
22 605 | application both to environmental reconstructions and diagenesis of sedimentary organic carbon.
23 606

24 607 | Gerard Versteegh combines organic geochemistry, palynology and palaeobotany to assess
25 608 | organic matter degradation, and, through this, to elucidate present and past environment and
26 609 | evolution. In 1995 received his PhD in Biology at Utrecht University on palynology and the
27 610 | onset of Northern Hemisphere ~~Glaciations~~glaciations. He ~~e~~Expanded his expertise with organic
28 611 | geochemistry at the Netherlands Institute for Sea Research. At the Université de Lille 1, France
29 612 | he was an invited Professor in 2007 and 2008 and obtained a prestigious Heisenberg Fellowship
30 613 | from the German Science Foundation in 2009. Currently he is at the Alfred-Wegener-Institute in
31 614 | Bremerhaven and the Centre for Marine Environmental Research, Bremen University. His
32 615 | interests include the macromolecular composition of palynomorphs, selective degradation of
33 616 | organic matter, the Paleozoic terrestrialisation, (sub)recent Mediterranean environmental change,
34 617 | proxy development, lipids, acritarchs and dinoflagellates.
35 618

36 619 | Fabienne Marret is a micropalaeontologist by training, with research interest in the field of
37 620 | Quaternary palaeoceanography and palaeoecology. She received her Ph.D. in 1994 from the
38 621 | University of Bordeaux, France. She studies marine sediments from around the world to interpret
39 622 | past environmental changes, based on vegetation tracers (pollen grains) and sea-surface
40 623 | conditions (dinoflagellate cysts). She is particularly interested in the causes of abrupt climate
41 624 | changes in the past, from the tropics to the poles.
42 625

43 626 | R. Eugene Turner is a faculty member at Louisiana State University. He received his Ph.D. in
44 627 | 1974 from the University of Georgia, USA. His research interests include coastal oceanography
45 628 | and wetlands.
46 629

47 630 | Nancy Rabalais is Executive Director and Professor of the Louisiana Universities Marine
48 631 | Consortium in Chauvin, Louisiana. Since the mid-1980s, Rabalais has been the driving force
49 632 | behind identifying and characterizing the dynamics of the large hypoxic region in the Gulf of
50 633 | Mexico, which receives excess nutrients from the Mississippi River. She serves on numerous
51 634 | boards and panels for federal agencies and national organizations. She has received numerous
52 635 | awards, most recently the John D. & Catherine T. MacArthur 'genius' award (2012). She
53 636 | graduated with a Ph.D. from the University of Texas in 1983.
54 637

638 Kazumi Matsuoka is a Professor Emeritus at Nagasaki University. ~~After retiring in~~ Although
639 retired since 2013, he continues scientific ~~works in~~ research on fossil and modern dinoflagellates
640 in particular cyst-motile form relationships of both naked and thecate dinoflagellates.

641 642 References

643
644 Adl SM, Simpson AGB, Farmer MA, Andersen RA, Anderson OR, Barta JR, Bowser SS,
645 Brugerolle G, Fensome RA, Fredericq S, et al. 2005. The new higher level classification of
646 Eukaryotes with emphasis on the taxonomy of Protists. *J Eukaryot Microbiol.* 52: 399–451.

647
648 Artzner DG, Dörhöfer G. 1978. Taxonomic note: *Lejeunecysta* nom. nov. pro *Lejeunia* Gerlach
649 1961 emend. Lentin and Williams 1976 - dinoflagellate cyst genus. *Can J Bot* 56: 1381–1382.

650
651 Baldwin RP. 1987. Dinoflagellate resting cysts isolated from sediments in Marlborough Sounds,
652 New Zealand. *New Zeal Mar Fresh.* 21: 543–553.

653
654 Balech E. 1974. El Genero "*Protoperidinium*" Bergh, 1881 (*Peridinium* Ehrenberg, 1831,
655 partim). *Revista Mus Argent Ci Nat, Bernardino Rivadavia Inst Nac Invest Ci Nat Bot.* 4: 1–79.

656
657 Balech E. 1988. Los dinoflagellados del Atlántico Sudoccidental. *Pub Esp Inst Español*
658 *Oceanografía* 1: 1–310.

659
660 Benedek PN. 1972. Phytoplanktonen aus dem Mittel- und Oberoligozän von Tönisberg
661 (Niederrheingebiet). *Palaeontogr Abt B* 137: 1–71.

662
663 Bergh RS. 1881. Der Organismus der Cilioflagellaten. Eine phylogenetische Studie. *Gegenbaurs*
664 *Morpholog Jahrb.* 7: 177–288.

665
666 Boc A, Diallo AB, Makarenkov V. 2012. T-REX: a web server for inferring, validating and
667 visualizing phylogenetic trees and networks. *Nucleic Acids Res.* 40: W573–W579.

668
669 Boessenkool K, Van Gelder M-J, Brinkhuis H, Troelstra SR. 2001. Distribution of organic-
670 walled dinoflagellate cysts in surface sediments from transects across the Polar Front offshore
671 southeast Greenland. *J Quaternary Sci.* 16: 661–666.

672
673 Bogus K, Harding IC, King A, Charles AK, Zonneveld K, Versteegh, GJM. 2012. The
674 composition of species of the *Apectodinium* complex (Dinoflagellata). *Rev Palaeobot Palynol.*
675 183: 21–31.

676
677 Bogus K, Mertens KNM, Lauwaert J, Harding IC, Vrielinck H, Zonneveld K, Versteegh, GJM.
678 2014. Differences in the chemical composition of organic-walled dinoflagellate resting cysts
679 from phototrophic and heterotrophic dinoflagellates. *J Phycol.* 50: 254–266.

680
681 Bolch CJS. 1997. The use of polytungstate for the separation and concentration of living
682 dinoflagellate cysts from marine sediments. *Phycologia* 37: 472–478.

Formatted: Font: Italic

Formatted: Font: Italic

- 1
2
3
4
5
6
7
8
9 684 Bradford MR. 1977. New species attributable to the dinoflagellate cyst genus *Lejeunia* Gerlach,
10 685 1961 emend. Lentin and Williams 1975. Grana 16: 45–59.
11 686
12 687 Bringué M, Pospelova V, Pak D. 2013. Seasonal production of organic-walled dinoflagellate
13 688 cysts in an upwelling system: a sediment trap study from the Santa Barbara Basin, California.
14 689 Mar Micropaleontol. 100: 34–51.
15 690
16 691 Bujak JP. 1984. Cenozoic dinoflagellate cysts and acritarchs from the Bering Sea and northern
17 692 North Pacific, D.S.D.P. Leg 19. Micropaleontology 30: 180–212.
18 693
19 694 Bujak JP, Davies EH. 1983. Modern and fossil Peridiniineae. AASP Contribution Series 13: 1–
20 695 204.
21 696
22 697 Bütschli O. 1885. Erster Band. Protozoa. 3. Unterabtheilung (Ordnung) Dinoflagellata. In: Dr.
23 698 H.G. Bronn's Klassen und Ordnungen des Thier-Reichs, wissenschaftlich dargestellt in Wort und
24 699 Bild. C.F. Leipzig und Heidelberg: Winter'sche Verlagshandlung; p. 906–1029.
25 700
26 701 Cárdenas G, Cabrera G, Taboada E, Miranda SP. 2004. Chitin characterization by SEM, FTIR,
27 702 XRD, and ¹³C cross polarization/mass angle spinning NMR. J Appl Polym Sci. 93: 1876–1885.
28 703
29 704 Cho H-J, Kim C-H, Moon C-H, Matsuoka K. 2003. Dinoflagellate cysts in recent sediments
30 705 from the southern coastal waters of Korea. Bot Mar. 46: 332–337.
31 706
32 707 Colthup NB, Daly LH, Wiberly SE. 1990. Introduction to Infrared and Raman Spectroscopy.
33 708 London: Academic Press Limited.
34 709
35 710 Daugbjerg N, Hansen G, Larsen J, Moestrup Ø. 2000. Phylogeny of some of the major genera of
36 711 dinoflagellates based on ultrastructure and partial LSU rDNA sequence data, including the
37 712 erection of three new genera of unarmoured dinoflagellates. Phycologia 39: 302–317.
38 713
39 714 de Leeuw JW, Versteegh GJM, van Bergen PF. 2006. Biomacromolecules of algae and plants
40 715 and their fossil analogues. Plant Ecol. 182: 209–233.
41 716
42 717 [De Schepper S, Head MJ, Louwye S. 2009. Pliocene dinoflagellate cyst stratigraphy,
43 718 palaeoecology and sequence stratigraphy of the Tunnel-Canal Dock, Belgium. Geol Mag 146:
44 719 92–112.](#)
45 720
46 721 de Vernal A, Londeix L, Mudie PJ, Harland R, Morzadec-Kerfourn M-T, Turon J-L, Wrenn JH.
47 722 1992. Quaternary organic-walled dinoflagellate cysts of the North Atlantic Ocean and adjacent
48 723 seas: ecostratigraphy and biostratigraphy. In: Head MJ, Wrenn JH, editors. Neogene and
49 724 Quaternary dinoflagellate cysts and acritarchs. Dallas, Texas: American Association of
50 725 Stratigraphic Palynologists Foundation; p. 289–328.
51 726
52 727 de Verteuil L, Norris G. 1992. Miocene Protoperidiniacean dinoflagellate cysts from the
53 728 Maryland and Virginia coastal plain. In: Head MJ, Wrenn JH, editors. Neogene and Quaternary

1
2
3
4
5
6
7
8
9
10
11
12
13
14
15
16
17
18
19
20
21
22
23
24
25
26
27
28
29
30
31
32
33
34
35
36
37
38
39
40
41
42
43
44
45
46
47
48
49
50
51
52
53
54
55
56
57
58
59
60

- 729 dinoflagellate cysts and acritarchs. Dallas, Texas: American Association of Stratigraphic
730 Palynologists Foundation; p. 391–430.
731
- 732 Faust MA. 2006. Creation of the subgenus *Testeria* Faust *subgen. nov. Protoperidinium* Bergh
733 from the SW Atlantic Ocean: *Protoperidinium novella* sp. nov. and *Protoperidinium concinna*
734 sp. nov. Dinophyceae. Phycologia 45: 1–9.
735
- 736 Fensome RA, Taylor FJR, Norris G, Sarjeant WAS, Wharton DI, Williams GL. 1993. A
737 classification of fossil and living dinoflagellates. Micropaleontology Special Publication 7: 1–
738 245.
739
- 740 Fukuyo Y, Takano H, Chihara M, Matsuoka K. 1990. Red tide organisms in Japan-An illustrated
741 taxonomic guide. In: Fukuyo Y, Takano H, Chihara M, Matsuoka, editors. Tokyo, Japan: Uchida
742 Rokakuho Co. Ltd. (In Japanese/English); 407 p.
743
- 744 Furio EE, Matsuoka K, Mizushima K, Baula I, Chan KW, Puyong A, Srivilai D, Sidharta, BR,
745 Fukuyo Y. 2006. Assemblage and geographical distribution of dinoflagellate cysts in surface
746 sediments of coastal waters of Sabah, Malaysia. Coastal Marine Science 30: 62–73.
747
- 748 Gómez F. 2012. A checklist and classification of living dinoflagellates (Dinoflagellata,
749 Alveolata). CICIMAR Oceanides 27: 65–140.
750
- 751 Gribble KE, Anderson DA. 2006. Molecular phylogeny of the heterotrophic dinoflagellates,
752 *Protoperidinium*, *Diplopsalis* and *Preperidinium* (Dinophyceae), inferred from large subunit
753 rDNA. J Phycol 42: 1081–1095.
754
- 755 Gu H, Liu T, Mertens KN. 2015. Cyst-theca relationship and phylogenetic positions of
756 *Protoperidinium* (Peridinales, Dinophyceae) species of the sections *Conica* and *Tabulata*.
757 Phycologia 54: 49–66.
758
- 759 Haeckel E. 1894. Systematische Phylogenie. Entwurf eines natürlichen Systems der Organismen
760 auf Grund ihrer Stammesgeschichte. 1. Theil: Systematische Phylogenie der Protisten und
761 Pflanzen: p. I–XV + 1–400, Georg Reimer (Berlin).
762
- 763 Hall TA. 1999. BioEdit: a user-friendly biological sequence alignment editor and analysis
764 program for Windows 95/98/NT. pp. 95–98.
765
- 766 Harland R. 1977. Recent and Late Quaternary (Flandrian and Devensian) dinoflagellate cysts
767 from marine continental shelf sediments around the British Isles. Palaeontogr Abt B 164: 87–
768 126.
769
- 770 Harland R. 1982. A review of recent and quaternary organic-walled dinoflagellate cysts of the
771 genus *Protoperidinium*. Palaeontology 25: 369–397.
772
773
774

- 1
2
3
4
5
6
7
8
9 775 [Head MJ, Norris G, Mudie PJ. 1989. 26. New species of dinocysts and a new species of acritarch](#)
10 776 [from the upper Miocene and lowermost Pliocene, ODP Leg 105, Site 646, Labrador Sea. In:](#)
11 777 [Srivastava SP, Arthur M, Clement B, et al., editors. Ocean Drilling Program, Proceedings,](#)
12 778 [Scientific Results, Leg 105, p. 453–466.](#)
13 779
14 780 Head MJ. 1993. Dinoflagellates, sporomorphs and other palynomorphs from the Upper Pliocene
15 781 St. Erth Beds of Cornwall, southwestern England. J Paleo. Memoir 31: 1–62.
16 782
17 783 Head MJ. (Ed.) 1994. A forum on Neogene and Quaternary dinoflagellate cysts: the edited
18 784 transcript of a round table discussion held at the Third Workshop on Neogene and Quaternary
19 785 Dinoflagellates; with taxonomic appendix. Palynology 17: 201–239. [Imprinted 1993]
20 786
21 787 [Head MJ, Norris G, Mudie PJ. 1989. 26. New species of dinocysts and a new species of acritarch](#)
22 788 [from the upper Miocene and lowermost Pliocene, ODP Leg 105, Site 646, Labrador Sea. In:](#)
23 789 [Srivastava SP, Arthur M, Clement B, et al., editors. Ocean Drilling Program, Proceedings,](#)
24 790 [Scientific Results, Leg 105, p. 453–466.](#)
25 791
26 792 [Head MJ, Riding JB, Eidvin T, Chadwick RA. 2004. Palynological and foraminiferal](#)
27 793 [biostratigraphy of \(Upper Pliocene\) Nordland Group mudstones at Sleipner, northern North Sea.](#)
28 794 [Mar Petrol Geol 21: 277–297.](#)
29 795
30 796 Hoppenrath M, Elbrächter M, Drebes G. 2009. Marine Phytoplankton. Selected
31 797 Microphytoplankton Species from the North Sea around Helgoland and Sylt. Kleine
32 798 Senckenberg-Reihe 49, 264 pp.
33 799
34 800 [Jiménez-Moreno G, Head MJ, Harzhauser M. 2006. Early and Middle Miocene dinoflagellate](#)
35 801 [cyst stratigraphy of the Central Paratethys, Central Europe. J Micropal 25: 113–139.](#)
36 802
37 803 Jörgensen E. 1912. Bericht über die von der schwedischen Hydrographisch- Biologischen
38 804 Kommission in den schwedischen Gewässern in den Jahren 1909-1910 eingesammelten
39 805 Planktonproben. Svenska Hydrogr-Biol Komm Skr. 4: 1–20.
40 806
41 807 Katoh K, Kuma K, Toh H, Miyata T. 2005. MAFFT version 5: improvement in accuracy of
42 808 multiple sequence alignment. Nucleic Acids Res. 33: 511–518.
43 809
44 810 Kawami H, Matsuoka K. 2009. A new cyst-theca relationship for *Protoperidinium parthenopes*
45 811 (Peridinales, Dinophyceae). Palynology 33: 11–18.
46 812
47 813 Kawami H, van Wezel R, Koeman RPT, Matsuoka K. 2009. *Protoperidinium tricingulatum* sp.
48 814 nov. (Dinophyceae), a new motile form of a round, brown, and spiny dinoflagellate cyst. Phycol
49 815 Res. 57: 259–267.
50 816
51 817 Kojima N, Seto K, Takayasu K, Nakamura M. 1994. Dinoflagellate cysts assemblage found in
52 818 the surface sediments of Lake Nakaumi, Western Japan. Laguna 1: 45–51.
53 819
54
55
56
57
58
59
60

1
2
3
4
5
6
7
8
9
10
11
12
13
14
15
16
17
18
19
20
21
22
23
24
25
26
27
28
29
30
31
32
33
34
35
36
37
38
39
40
41
42
43
44
45
46
47
48
49
50
51
52
53
54
55
56
57
58
59
60

- 820 Krepakevich A, Pospelova V. 2010. Tracing the influence of sewage discharge on coastal bays
821 of Southern Vancouver Island (BC, Canada) using sedimentary records of phytoplankton. Cont
822 Shelf Res. 30: 1924–1940.
- 823
824 Lewis J, Dodge JD, Tett P. 1984. Cyst-theca relationships in some *Protopteridinium* species
825 (Peridinales) from Scottish sea lochs. Journal of Micropalaeontology 3: 25–34.
- 826
827 Lewis J, Dodge JD. 1987. The cyst-theca relationship of *Protopteridinium americanum* (Gran &
828 Braarud) Balech. Journal of Micropalaeontology 6: 113–121.
- 829
830 Li Z, Matsuoka K, Shin HH, Kobayashi S, Shin K, Lee T, Han M-S, 2015. *Brigantedinium*
831 *majusculum* is the cyst of *Protopteridinium sinuosum* (Protopteridiniaceae, Dinophyceae).
832 Phycologia 54: 517–529.
- 833
834 Liu T, Gu H, Mertens KN, Lan D. 2014. A new dinoflagellate species *Protopteridinium*
835 *haizhouense* sp. nov. (Peridinales, Dinophyceae), its cyst-theca relationship and phylogenetic
836 position within the *Monovela* group. Phycol Res. 62: 109–124.
- 837
838 Liu T, Mertens KN, Ribeiro S, Ellegaard M, Matsuoka H, Gu H. 2015a. Cyst-theca relationships
839 and phylogenetic positions of Peridinales (Dinophyceae) with two anterior intercalary plates,
840 with description of *Archaeperidinium bailongense* n. sp. and *Protopteridinium fuzhouense* n. sp.
841 Phycol Res. 63: 134–151.
- 842
843 Liu T, Mertens KN, Gu H. 2015b. Cyst-theca relationship and phylogenetic positions of the
844 diplopsalioideans (Peridinales, Dinophyceae), with description of *Niea* and *Qia* gen. nov.
845 Phycologia 54: 210–232.
- 846
847 Louwye S, Mertens KN, Vercauteren D. 2008. New dinoflagellate cysts from the Miocene of the
848 Porcupine Basin, offshore southwest Ireland. Palynology 32: 131–142.
- 849
850 Matsuoka K. 1982. *Protopteridinium pentagonum* (Gran) Balech. In: the working party in
851 taxonomy in the Akashiwo Kenyukai, editors. Synopsis of Red-tide organisms. Sheet no. 108 [In
852 Japanese].
- 853
854 Matsuoka K. 1987. Organic-walled dinoflagellate cysts from surface sediments of Akkeshi Bay
855 and Lake Saroma, North Japan. Bulletin Faculty of Liberal Arts, Nagasaki University (Natural
856 Science) 28: 35–123.
- 857
858 Matsuoka K. 1992. Peridiniacean cyst genus *Xandarodinium* in the Miocene Kaminoyama
859 Formation in the western part of Zao Volcano, Yamagata, north Japan. In: Ishizaki K, Saito T.,
860 editors. Centenary of Japanese Micropaleontology. Tokyo, Japan: Terra Scientific Publishing
861 Company; p.449-455.
- 862
863 Matsuoka K, Head MJ. 2013. Clarifying cyst–motile stage relationships in dinoflagellates. In:
864 Lewis JM, Marret F, Bradley L., editors. Biological and Geological Perspectives of

- 1
2
3
4
5
6
7
8
9 865 Dinoflagellates. London: The Micropalaeontological Society, Special Publications. Geological
10 866 Society, p. 325–350.
11 867
12 868 Matsuoka K, Kawami H, Nagai S, Iwataki M, Takayama H. 2009. Re-examination of cyst-motile
13 869 relationships of *Polykrikos kofoidii* Chatton and *Polykrikos schwartzii* Bütschli (Gymnodiniales,
14 870 Dinophyceae). Rev Palaeobot Palynol 154: 79–90.
15 871
16 872 Matsuoka K, Joyce LB, Kotani Y, Matsuyama Y. 2003. Modern dinoflagellate cysts in
17 873 hypertrophic coastal waters of Tokyo Bay, Japan. J Plankton Res. 25: 1461–1470.
18 874
19 875 Mertens KN, Yamaguchi A, Kawami H, Ribeiro S, Leander BS, Price AM, Pospelova V,
20 876 Ellegaard, M, Matsuoka K. 2012a. *Archaeperidinium saanichi* sp. nov.: A new species based on
21 877 morphological variation of cyst and theca within the *Archaeperidinium minutum* Jörgensen 1912
22 878 species complex. Mar Micropaleontol. 96: 48–62.
23 879
24 880 Mertens KN, Bringué M, Van Nieuwenhove N, Takano Y, Pospelova V, Rochon A, de Vernal
25 881 A, Radi T, Dale B, Patterson RT, Weckström K, Andrén E, Louwye S, Matsuoka K. 2012b.
26 882 Process length variation of the cyst of the dinoflagellate *Protoceratium reticulatum* in the North
27 883 Pacific and Baltic-Skagerrak region: calibration as an annual density proxy and first evidence of
28 884 pseudo-cryptic speciation. J Quaternary Sci. 27: 734–744.
29 885
30 886 Mertens KN, Yamaguchi A, Takano Y, Pospelova V, Head MJ, Radi T, Pieńkowski A, de
31 887 Vernal A, Kawami H, Matsuoka K. 2013. A new heterotrophic dinoflagellate from the
32 888 Northeastern Pacific, *Protoperidinium fukuyoi*: cyst-theca relationship, phylogeny, distribution
33 889 and ecology. J Eukaryot Microbiol. 60: 545–563.
34 890
35 891 Mertens KN, Takano Y, Yamaguchi A, Gu H, Bogus K, Kremp A, Bagheri S, Matishov G,
36 892 Matsuoka K. 2015. The molecular characterization of the enigmatic dinoflagellate *Kolkwitzia*
37 893 *acuta* reveals an affinity to the *Excentrica* section of the genus *Protoperidinium*. Syst Biodivers.
38 894 doi:10.1080/14772000.2015.1078855.
39 895
40 896 Nehring S. 1997. Dinoflagellate resting cysts from German coastal sediments. Bot Mar. 40: 307–
41 897 324.
42 898
43 899 Orr RJS, Murray SA, Stüken A, Rhodes L, Jakobsen KS. 2012. When naked became armored:
44 900 An eight-gene phylogeny reveals monophyletic origin of theca in dinoflagellates. PloS one 7:
45 901 e50004.
46 902
47 903 Pascher A. 1914. Über Flagellaten und Algen. Berichte der Deutschen Botanischen
48 904 Gesellschaft 32: 136–160.
49 905
50 906 Posada D. 2008. jModelTest: phylogenetic model averaging. Mol Biol Evol. 25: 1253–1256.
51 907
52 908 Pospelova V, Chmura GL, Walker HA. 2004. Environmental factors influencing spatial
53 909 distribution of dinoflagellate cyst assemblages in shallow lagoons of southern New England
54 910 (USA). Rev Palaeobot Palynol. 128:7–34.

Formatted: Font: Italic

Formatted: Font: Italic

1
2
3
4
5
6
7
8
9
10
11
12
13
14
15
16
17
18
19
20
21
22
23
24
25
26
27
28
29
30
31
32
33
34
35
36
37
38
39
40
41
42
43
44
45
46
47
48
49
50
51
52
53
54
55
56
57
58
59
60

- 911
912 Pospelova V, de Vernal A, Pedersen TF. 2008. Distribution of dinoflagellate cysts in surface
913 sediments from the northeastern Pacific Ocean (43–25 degrees N) in relation to sea-surface
914 temperature, salinity, productivity and coastal upwelling. *Mar Micropaleontol.* 68: 21–48.
915
916 Price AM, Pospelova V. 2011. High-resolution sediment trap study of organic-walled
917 dinoflagellate cyst production and biogenic silica flux in Saanich Inlet (BC, Canada). *Mar*
918 *Micropaleontol.* 80: 18–43.
919
920 Radi T, de Vernal A. 2004. Dinocyst distribution in surface sediments from the northeastern
921 Pacific margin (40–60°N) in relation to hydrographic conditions, productivity and upwelling.
922 *Rev Palaeobot Palynol.* 128: 169–193.
923
924 Reid P. 1977. Peridiniacean and glenodiniacean dinoflagellate cysts from the British Isles. *Nova*
925 *Hedwigia* 29: 429–463.
926
927 Ribeiro S, Lundholm N, Amorim A, Ellegaard M. 2010. *Protoperidinium minutum*
928 (Dinophyceae) from Portugal: cyst-theca relationship and phylogenetic position on the basis of
929 single-cell SSU and LSU rDNA sequencing. *Phycologia* 49: 48–63.
930
931 Rochon A, de Vernal A, Turon J-L, Matthiessen J, Head MJ. 1999. Distribution of recent
932 dinoflagellate cysts in surface sediments from the North Atlantic Ocean and adjacent seas in
933 relation to sea-surface parameters. *AASP Contribution Series*, 35, 146 pp.
934
935 Ronquist F, Huelsenbeck JP. 2003. MrBayes 3: Bayesian phylogenetic inference under mixed
936 models. *Bioinformatics* 19: 1572–1574.
937
938 Sarai C, Kawami H, Matsuoka K. 2013. Two new species formally attributed to *Protoperidinium*
939 *oblongum* (Aurivillius) Park et Dodge (Peridinales, Dinophyceae): Evidence from cyst
940 incubation experiments. *Rev Palaeobot Palynol.* 192: 103–118.
941
942 Scholin CA, Herzog M, Sogin M, Anderson DM. 1994. Identification of group- and strain-
943 specific genetic markers for globally distributed *Alexandrium* (Dinophyceae). II. Sequence
944 analysis of a fragment of the LSU rRNA gene. *J Phycol.* 30: 999–1011.
945
946 Shin HH, Yoon YH, Kim Y-O, Matsuoka K. 2011. Dinoflagellate Cysts in Surface Sediments
947 from Southern Coast of Korea. *Estuaries and Coasts* 34: 712–725.
948
949 [Soliman A, Ćorić S, Head MJ, Piller W, El Beialy SY, 2012. Lower and Middle Miocene](#)
950 [biostratigraphy, Gulf of Suez, Egypt, based on dinoflagellate cysts and calcareous nannofossils,](#)
951 [Palynology 36: 1–42.](#)
952
953 Stamatakis A. 2006. RAxML-VI-HPC: maximum likelihood-based phylogenetic analyses with
954 thousands of taxa and mixed models. *Bioinformatics* 22: 2688–2690.
955
956 Taylor F. 1980. On dinoflagellate evolution. *BioSystems* 13: 65–108.

Formatted: Font: 12 pt

Formatted: Font: 12 pt

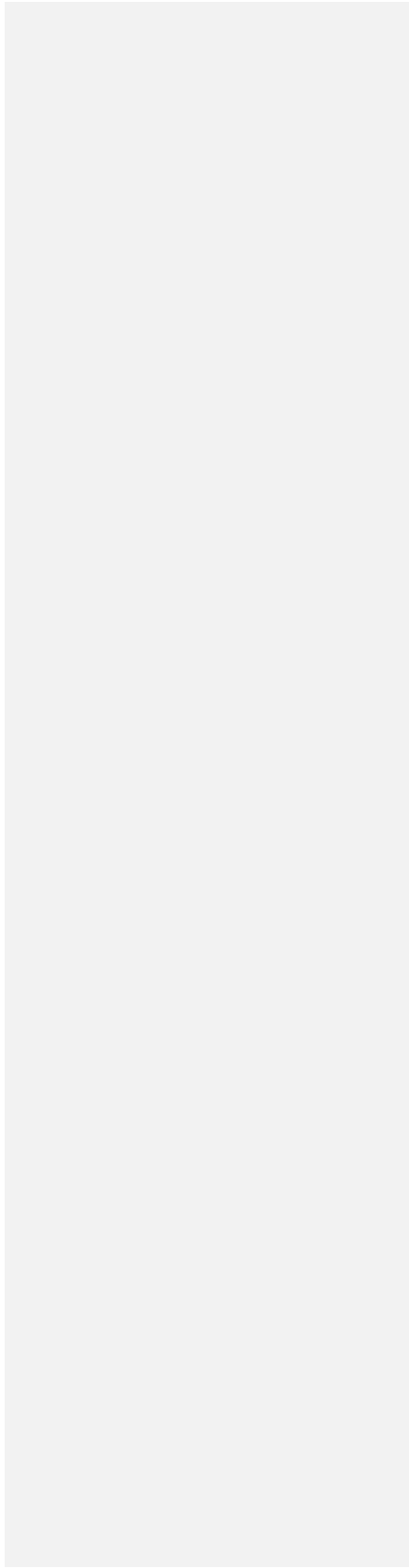
Formatted: Font: 12 pt

1
2
3
4
5
6
7
8
9
10
11
12
13
14
15
16
17
18
19
20
21
22
23
24
25
26
27
28
29
30
31
32
33
34
35
36
37
38
39
40
41
42
43
44
45
46
47
48
49
50
51
52
53
54
55
56
57
58
59
60

- 957
958 Verleye T, Pospelova V, Mertens KN, Louwe S. 2011. The geographical distribution and
959 (palaeo)ecology of *Selenopemphix undulata* sp. nov., a new late Quaternary dinoflagellate cyst
960 from the Pacific Ocean. *Mar Micropaleontol.* 78: 65–83.
961
- 962 Versteegh GJM, Blokker P, Bogus K, Harding IC, Lewis J, Oltmanns S, Rochon A, Zonneveld
963 KAF. 2012. Flash pyrolysis and infrared spectroscopy of cultured and sediment derived
964 *Lingulodinium polyedrum* (Dinoflagellata) cyst walls. *Org Geochem.* 43: 92–102.
965
- 966 Wall D, Dale B. 1968. Modern dinoflagellate cysts and evolution of the Peridinales.
967 *Micropaleontology* 14: 265–304.
968
- 969 Wang Z, Matsuoka K, Qi Y, Chen J. 2004. Dinoflagellate cysts in recent sediments from Chinese
970 coastal waters. *Marine Ecology* 25: 289–311.
971
- 972 Yamaguchi A, Kawamura H, Horiguchi T. 2006. A further phylogenetic study of the
973 heterotrophic dinoflagellate genus, *Proto-peridinium* (Dinophyceae) based on small and large
974 subunit ribosomal RNA gene sequences. *Phycol Res.* 54: 317–329.
975
- 976 Yamaguchi A, Kawamura H, Horiguchi T. 2007. The phylogenetic position of an unusual
977 *Proto-peridinium* species, *P. bipes* (Peridinales, Dinophyceae), based on small and large subunit
978 ribosomal RNA gene sequences. *Phycologia* 46: 270–276.
979
- 980 Yamaguchi A, Hoppenrath M, Pospelova V, Horiguchi T, Leander BS. 2011. Molecular
981 phylogeny of the marine sand-dwelling dinoflagellate *Herdmania litoralis* and an emended
982 description of the closely related planktonic genus *Archaeoperidinium* Jörgensen. *Eur J Phycol.*
983 46: 98–112.
984
- 985 Yang CQ, Xu Y, Wang D. 1996. FT-IR spectroscopy study of the polycarboxylic acids used for
986 paper wet strength improvement. *Ind Eng Chem Res.* 35: 4037–4042.
987
988

1
2
3
4
5
6
7
8
9
10
11
12
13
14
15
16
17
18
19
20
21
22
23
24
25
26
27
28
29
30
31
32
33
34
35
36
37
38
39
40
41
42
43
44
45
46
47
48
49
50
51
52
53
54
55
56
57
58
59
60

989



990 Tables

991

992 Table 1. List of species belonging to the genus *Trinovantedinium*, their biostratigraphical ranges and dimensions.

993

| Species name | Biostratigraphical range | Length (excluding processes) (µm) | Width (excluding processes) (µm) | Length of processes (µm) | Measurements from |
|--|---|-----------------------------------|----------------------------------|--------------------------|---------------------------|
| <i>Trinovantedinium applanatum</i> (Bradford 1977) Bujak and Davies 1983 | middle Pleistocene (Mudie 1989) - recent (see Rochon et al. 1999 for remarks) | 53–87 | 47–74 | max 5 | Bradford 1977 |
| | | 54–80 | 54–80 | max 5–7 | Reid 1977 |
| <i>Trinovantedinium sterthense</i> Head 1993a | late Pliocene early Pleistocene (Head 1993a) | 41(50.0)61 | 45(49.6)53 | 4.5(5.5)7.0 | Head 1993a |
| <i>Trinovantedinium variabile</i> (Bujak 1984) de Verteuil and Norris 1992 | late Miocene (Bujak 1984) — recent (e.g., Radi & de Vernal 2004; Price & Pospelova 2011) | 45–53 | 44–50 | 4–6.5 | Bujak 1984 |
| <i>Trinovantedinium harpagonium</i> de Verteuil and Norris 1992 | middle Miocene (late Miocene (de Verteuil & Norris 1992) Jimenez-Moreno et al. 2006) — late Pliocene (De Schepper et al. 2009) | 52(60)78 | 48(59)68 | 8–16 | de Verteuil & Norris 1992 |
| <i>Trinovantedinium glorianum</i> (Head et al. 1989) de Verteuil and Norris 1992 | early Miocene (Louwye et al. 2007) — early Pleistocene (Head et al. 2004) | 58(68)73 | 52(63)70 | 2–3 | de Verteuil & Norris 1992 |
| <i>Trinovantedinium ferruginomatum</i> de Verteuil and Norris 1992 | late Miocene (de Verteuil & Norris 1992) — early Pliocene (De Schepper et al. 2009) | 30(39)55 | 30(39)48 | 3–6 | de Verteuil & Norris 1992 |
| <i>Trinovantedinium papula</i> de Verteuil and Norris 1992 | late Miocene (de Verteuil & Norris 1992) | 50(65)75 | 48(57)70 | 3–6 | de Verteuil & Norris 1992 |
| <i>Trinovantedinium pallidifulum</i> Matsuoka 1987 | mid Miocene (de Verteuil & Norris 1992 ¹) — recent (Matsuoka 1987) | 52.2–70.8 | 56.0–63.4 | 2.5 | Matsuoka 1987 |
| | | 43.0(58.5)68.4 | 46.3(56.5)63.9 | 1.1(1.8)2.7 | This study |
| <i>Trinovantedinium henrietii</i> Louwye et al. 2008 | mid Miocene (Louwye et al. 2008) | 81(89)99 | 61(75)84 | 5(7)10 | Louwye et al. 2008 |
| <i>Trinovantedinium?</i> <i>xylochoporum</i> de Verteuil and Norris 1992 | lower Miocene (Soliman et al. 2012) — middle Miocene (Jimenez-Moreno et al. 2006) mid Miocene (de Verteuil & Norris 1992) | 36(51)66 | 38(45)62 | 8–20 | de Verteuil & Norris 1992 |
| <i>Trinovantedinium boreale</i> Bujak 1984 | late Paleocene — late Oligocene (Kurita & Matsuoka 1993; see Head 1994 for discussion) | 42–65 | 42–63 | 7–15 | Bujak 1984 |

Formatted: French (France)

Formatted: English (U.K.)

Formatted: English (U.S.)

Formatted: English (U.K.)

Formatted: Font: Not Italic

Formatted: English (U.K.)

¹Our interpretation of the "undefined protoperidiniacean species" depicted in de Verteuil & Norris, plate 2, figs. 9–12.

Table 2. Sampling stations with details on the collection site, relative abundance (%) and how the sample was used in this study.

994

| Station | Location | Latitude (°N) | Longitude (°E) | Water depth (m) | Sampling data | Salinity (psu) | Temperature (°C) | Type of core | Sampled by* | Relative abundance (%) | Notes |
|-----------------------|------------------------|---------------|----------------|-----------------|---------------|----------------|------------------|---------------|-------------|------------------------|--|
| Heslwall, Dee Estuary | UK | 53,32 | -3,12 | 0 | 6/02/14 | NA | NA | Hand sampling | FM | NA | Germination experiment |
| Wadden Sea st. 1 | Northern Germany | 53,72 | 7,97 | 0 | 29/02/12 | NA | NA | Hand sampling | GV, KZ, KNM | NA | Germination experiment |
| Vinga SW | Kattegat | 57,55 | 11,53 | 77,5 | 1994 | NA | NA | Boxcore | AG | NA | Palynological study |
| BV3 | La Vilaine Bay, France | 47,48 | -2,44 | 6 | 1/04/10 | NA | NA | Boxcore | EG | NA | Palynological study |
| C6B | Gulf of Mexico | 28,87 | -90,47 | 18,4 | 28/07/08 | 22,17 | 30,54 | Boxcore | GT, NR | 0,8 | Palynological study |
| E2A | Gulf of Mexico | 28,74 | -91,25 | 15,2 | 28/07/08 | 16,14 | 29,7 | Boxcore | GT, NR | 0,6 | Palynological study |
| G3 | Gulf of Mexico | 28,98 | -92,00 | 20,2 | 28/07/08 | 21,51 | 30,45 | Boxcore | GT, NR | 0,9 | Palynological study |
| J4 | Gulf of Mexico | 29,29 | -93,08 | 15 | 25/07/08 | 27,99 | 30,52 | Boxcore | GT, NR | 0,8 | Palynological study |
| A'2 | Gulf of Mexico | 29,09 | -89,50 | 11,2 | 27/07/14 | 8,60 | 31,45 | Boxcore | GT, NR | 0,3 | Palynological study |
| A'3 | Gulf of Mexico | 29,03 | -89,53 | 13,2 | 27/07/14 | 13,60 | 30,99 | Boxcore | GT, NR | 1,7 | Palynological study |
| A'4 | Gulf of Mexico | 28,98 | -89,57 | 33,7 | 27/07/14 | 15,15 | 30,90 | Boxcore | GT, NR | 0,6 | Palynological study |
| A'5 | Gulf of Mexico | 28,95 | -89,58 | 63,9 | 27/07/14 | 17,73 | 30,19 | Boxcore | GT, NR | 1,7 | Palynological study |
| A2 | Gulf of Mexico | 29,24 | -89,75 | 13,5 | 28/07/14 | 25,00 | 30,00 | Boxcore | GT, NR | 1,2 | Palynological study |
| A5 | Gulf of Mexico | 29,07 | -89,75 | 30,5 | 28/07/14 | 25,30 | 29,70 | Boxcore | GT, NR | 1,2 | Palynological study |
| A7 | Gulf of Mexico | 28,94 | -89,75 | 53,20 | 28/07/14 | 24,70 | 29,90 | Boxcore | GT, NR | 2,0 | Germination experiment / Palynological study |
| B4 | Gulf of Mexico | 29,03 | -90,12 | 18,5 | 28/07/14 | 28,09 | 29,55 | Boxcore | GT, NR | 3,8 | Palynological study |
| C6C | Gulf of Mexico | 28,87 | -90,49 | 19,80 | 28/07/14 | 23,40 | 29,40 | Boxcore | GT, NR | 1,8 | Single-cell PCR / Palynological study |
| D3 | Gulf of Mexico | 28,72 | -90,83 | 17,8 | 29/07/14 | 15,05 | 30,83 | Boxcore | GT, NR | 2,4 | Palynological study |
| F0 | Gulf of Mexico | 29,27 | -91,62 | 8,0 | 31/07/14 | 23,20 | 31,30 | Boxcore | GT, NR | 3,7 | Palynological study |
| F3 | Gulf of Mexico | 28,88 | -91,62 | 19,9 | 30/07/14 | 29,15 | 29,92 | Boxcore | GT, NR | 1,5 | Palynological study |
| F6 | Gulf of Mexico | 28,58 | -91,62 | 39,6 | 30/07/14 | 30,02 | 29,51 | Boxcore | GT, NR | 0,8 | Palynological study |
| I4 | Gulf of Mexico | 29,18 | -92,75 | 20,8 | 1/08/14 | 32,40 | 30,00 | Boxcore | GT, NR | 0,3 | Palynological study |
| K4 | Gulf of Mexico | 29,33 | -93,42 | 17,3 | 1/08/14 | 31,74 | 29,92 | Boxcore | GT, NR | 0,8 | Palynological study |
| P6 | Gulf of Mexico | 29,00 | -93,71 | 20,0 | 1/08/14 | 33,61 | 30,08 | Boxcore | GT, NR | 0,3 | Palynological study |
| SR8 | Lake Saroma | 44,09 | 143,52 | ca. 7 | July 1980 | 33-33.2 | 0-15 | TFO corer | YF | 0,5 | Palynological study |

1
2
3
4
5
6
7
8
9
10
11
12
13
14
15
16
17
18
19
20
21
22
23
24
25
26
27
28
29
30
31
32
33
34
35
36
37
38
39
40
41
42
43
44
45
46
47
48
49

| | | | | | | | | | | | |
|-----------------------|---------------------------------|--------|---------|-------|-----------|---------------|----------------------------|----------------------|--------|---------|---------------------|
| AK2 | Akkeshi Bay, Japan | 43,02 | 144,47 | ca. 6 | July 1980 | 32.6-33 | 1.5(winter)- 14(summer) | TFO corer | YF | 0.5-1.8 | Palynological study |
| AB40 | Ariake Sound, Japan | 33,08 | 130,28 | 10,9 | 7/06/05 | 20.0- 30.2 | 9.2-28.5 | TFO corer | KM | NA | Palynological study |
| Tkb8 | Tokyo Bay, Japan | 35,27 | 139,45 | ca.12 | 1/08/99 | 26.8- 30.5 | 10.4-30.1 | KK type corer | RV | NA | Palynological study |
| Nagayo-Ura | Omura Bay, Japan | 32,51 | 129,52 | 11 | June 2004 | 30.8- 33.4 | 9.5-30.5 | sediment trap | HK, KM | NA | Palynological study |
| YJ1 | Yeoja Bay, Korea | 34,42 | 127,31 | 11 | May 2006 | NA | NA | Scuba diver | KM, HC | NA | Palynological study |
| D1 | Deukryang Bay, Korea | 34,40 | 127,11 | 10 | 1/04/01 | NA | NA | Gravity corer | HC | NA | Palynological study |
| Casino coast | Brazil | -32,12 | -52,10 | ca.10 | 7/03/97 | NA | NA | TFO corer | KM | NA | Palynological study |
| Saanich Inlet st. S13 | Vancouver Island, BC, Canada | 48,75 | -123,61 | 60 | 24/05/07 | 28,5 | 11,3 | Petite Ponar Grab | VP | NA | Palynological study |

995 * AG = Anna Godhe, EG = Evelyne Goubert, FM = Fabienne Marret, GV= Gerard Versteegh, GT = Gene Turner, HC = Hyun-Jin
 996 Cho, HK = Hisae Kawami, KM = Kazumi Matsuoka, KNM = Kenneth Neil Mertens, KZ = Karin Zonneveld, NR = Nancy Rabalais,
 997 RV = R/V Shirafuji-Maru, VP = Vera Pospelova, YF = Yasuo Fukuyo

998
999

1000

1001 Supplementary table 1. Sampling stations with details on latitude, longitude and water depth.

| Name of station | Locality | Latitude (°N) | Longitude (°E) | Water depth (m) | Reference |
|----------------------|------------------------|---------------|----------------|-----------------|----------------------|
| Akkeshi Bay AK1 | Hokkaido, Japan | 43,04 | 144,83 | 25 | Matsuoka 1987 |
| Akkeshi Bay AK2 | Hokkaido, Japan | 43,02 | 144,79 | 25 | Matsuoka 1987 |
| Akkeshi Bay AK3 | Hokkaido, Japan | 42,99 | 144,79 | 25 | Matsuoka 1987 |
| Akkeshi Bay AK4 | Hokkaido, Japan | 42,95 | 144,86 | 25 | Matsuoka 1987 |
| Saroma lake SR8 | Hokkaido, Japan | 44,14 | 143,86 | 16 | Matsuoka 1987 |
| 6 | Lake Nakaumi, Japan | 35,52 | 134,08 | NA | Kojima et al. 1994 |
| 8 | Lake Nakaumi, Japan | 35,52 | 134,08 | NA | Kojima et al. 1994 |
| 24 | Lake Nakaumi, Japan | 35,52 | 134,08 | NA | Kojima et al. 1994 |
| 25 | Lake Nakaumi, Japan | 35,52 | 134,08 | NA | Kojima et al. 1994 |
| 26 | Lake Nakaumi, Japan | 35,52 | 134,08 | NA | Kojima et al. 1994 |
| TKB-6 | Tokyo Bay, Japan | 35,50 | 139,83 | NA | Matsuoka et al. 2003 |
| D1 | South of South Korea | 34,67 | 127,18 | 10 | Cho et al. 2003 |
| 4 | Chinese coast | 22,56 | 114,51 | 6 | Wang et al. 2004 |
| Kuala Penyu Lagoon 1 | Sabah, Malaysia | 5,53 | 115,62 | NA | Furio et al. 2006 |
| Kuala Penyu Lagoon 2 | Sabah, Malaysia | 5,57 | 115,60 | NA | Furio et al. 2006 |
| YJB1 | Yeoja Bay, South Korea | 34,78 | 127,50 | NA | Shin et al. 2011 |
| YJB2 | Yeoja Bay, South Korea | 34,74 | 127,50 | NA | Shin et al. 2011 |
| YJB3 | Yeoja Bay, South Korea | 34,71 | 127,50 | NA | Shin et al. 2011 |
| YJB4 | Yeoja Bay, South Korea | 34,67 | 127,51 | NA | Shin et al. 2011 |
| YJB6 | Yeoja Bay, South Korea | 34,50 | 127,59 | NA | Shin et al. 2011 |
| YJB8 | Yeoja Bay, South Korea | 34,43 | 127,70 | NA | Shin et al. 2011 |
| GMB3 | Gamak Bay, South Korea | 34,60 | 127,70 | NA | Shin et al. 2011 |

1
2
3
4
5
6
7
8
9
10
11
12
13
14
15
16
17
18
19
20
21
22
23
24
25
26
27
28
29
30
31
32
33
34
35
36
37
38
39
40
41
42
43
44
45
46
47
48
49
50
51
52
53
54
55
56
57
58
59
60

Figure captions

Figure 1. Map showing locations where *Trinovantedinium pallidifulum* was found in this study (red circles) and in previous studies (blue circles) (see Table 1 and Supplementary Table 1 for respective sample localities).

Figure 2. Drawings of *Protoperidinium louisianensis* n. sp. A). Ventral view. B). Dorsal view.

Figure 3. Molecular phylogeny. A phylogenetic tree using Bayesian inference inferred from LSU rDNA sequences based on new sequence data for *Protoperidinium louisianensis* n. sp. from the Gulf of Mexico and *Selenopemphix undulata* from Brentwood Bay, BC, Canada. The ML bootstrap support values (ML) over 50 and Bayesian posterior probabilities (PP) over 0.7 are shown at the nodes (ML/PP). The black circles indicate maximal support. Clades are labeled and marked with vertical lines on the right, with dashed lines indicating sections of the *Protoperidinium sensu stricto* clade. The scale bar represents inferred evolutionary distance in changes/site. New sequences obtained in this study are indicated in bold font.

Figure 4. *Trinovantedinium pallidifulum* (German Wadden Sea) cyst wall FTIR spectrum in comparison with other cysts produced by heterotrophic dinoflagellates. The spectra from *D. caperatum*, *Brigantedinium* sp., cysts of *Polykrikos- kofoidii sensu Matsuoka et al. (2009)* and *Polykrikos- schwartzii sensu Matsuoka et al. (2009)* are modified from Bogus et al. (2014).

Plate captions

Plate 1. Figures 1–9. Different views of single specimen of motile stage of *Protoperidinium louisianensis* germinated from cyst depicted in Figures 10–15, and isolated from the Northern Gulf of Mexico. 1. General shape of cell. 2. Ventral view. 3. Lateral view. 4. Dorsal view showing the second intercalary plate (2a). 5. Lateral view. 6. Lateral view. 7. Ventral view showing sulcal area. 8. Dorsal view. 9. Ventral view of hypotheca. Figures 10–15. Cyst stage of *Protoperidinium louisianensis*, corresponding to *Trinovantedinium pallidifulum*, with motile stage depicted in Figures 1–9. 10. Ventral view. 11. Cross section. 12. Dorsal view showing operculum. 13. Peritabular distribution of processes. 14–15. Ventral view showing process distribution on the hypotheca. All scale bars = 10 μ m.

Plate 2. Figures 1–9. Motile stage of *Protoperidinium louisianensis* germinated from cyst depicted in Figures 10–15, isolated from the Northern Gulf of Mexico. 1. Cross section showing general shape and cell contents. 2. Ventral view. 3. Ventral view showing shape of the first apical plate. 4. Focus on the apical pore. 5. Dorsal view showing shape of second intercalary plate (2a). 6. Lateral view. 7. Ventral view showing sulcal area. 8. Dorsal view. 9. View of dorsal side of hypotheca. Figures 10–15. Cyst stage of *Protoperidinium louisianensis*, corresponding to *Trinovantedinium pallidifulum*, with motile stage depicted in Figures 1–9. 10. General shape of cyst. 11. Ventral view showing peritabular distribution of processes. 12. Ventral view showing presence of 2 flagellar scars. 13. Lateral view. 14. Dorsal view showing operculum. 15. Dorsal view of hypotheca showing presence of striations on this specimen. All scale bars = 10 μ m.

1
2
3
4
5
6
7
8
9
10
11
12
13
14
15
16
17
18
19
20
21
22
23
24
25
26
27
28
29
30
31
32
33
34
35
36
37
38
39
40
41
42
43
44
45
46
47
48
49
50
51
52
53
54
55
56
57
58
59
60

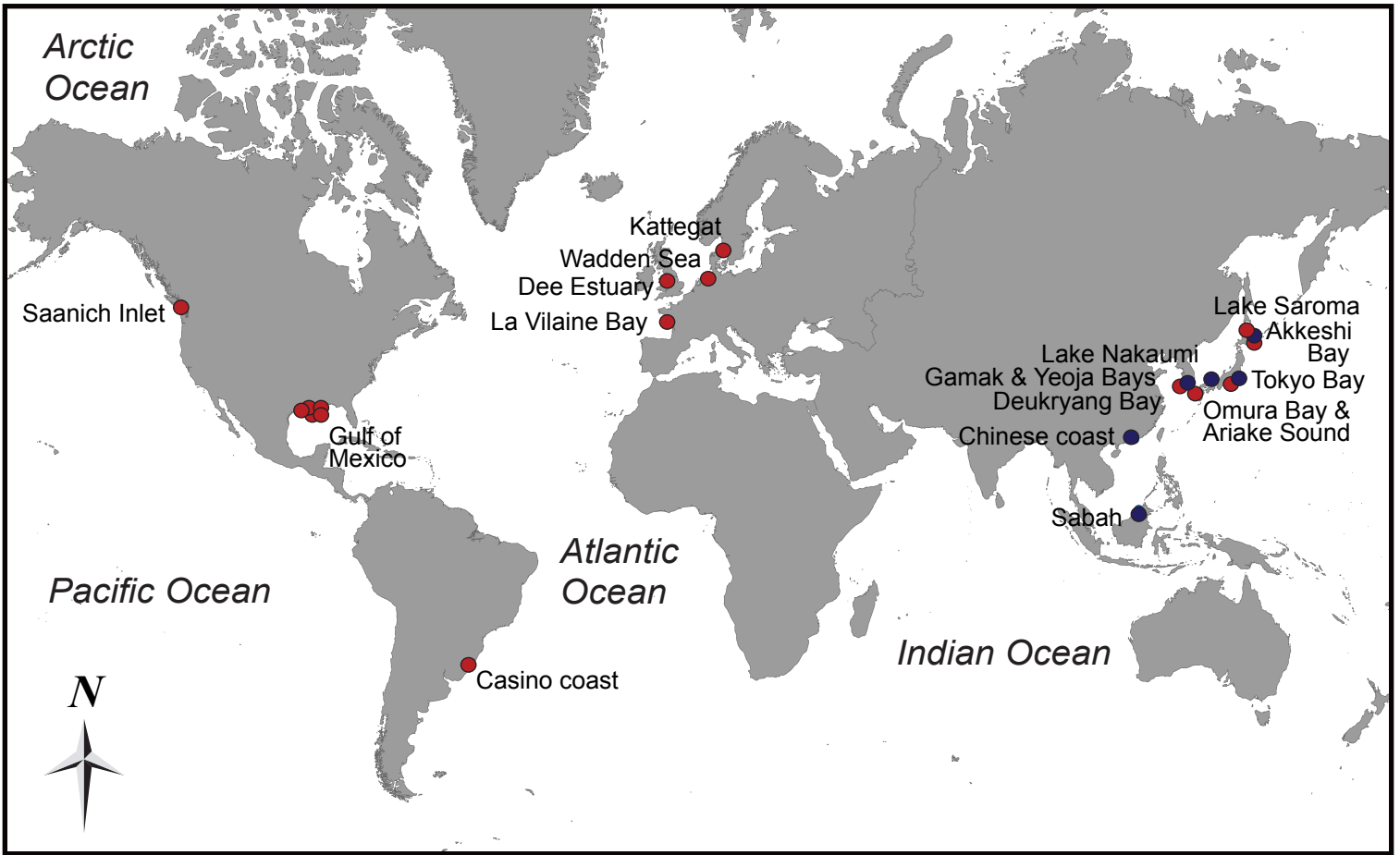
1047 Plate 3. Figures 1–12. *Trinovantedinium pallidifulum* from German Wadden Sea. 1–3. Cyst
1048 with cell contents from St. 1. 4–8. Different orientations of germinated specimen. 9–12. Other
1049 specimen). 9. Apical pore. Figures 13–16. Holotype of *Trinovantedinium pallidifulum*. Slide no.
1050 AK2–2 (87.4/27.6); Sample no. AK2, ~~Recent~~ modern sediment in Akkeshi Bay, Hokkaido,
1051 North Japan (Matsuoka 1987). All scale bars = 10 μ m.

1052
1053 Plate 4. Figures 1–12. *Trinovantedinium applanatum*. 1–4. High focus to low focus of single
1054 specimen from 11–12 cm depth in core po287-39-1B (37.75°N, 8.87°W, 92 m water depth, Mira,
1055 Portugal). 5–6, 8–10. Different orientations of single specimen isolated from the German
1056 Wadden Sea (location shown in Table 2). 7. Other specimen from the German Wadden Sea. 11–
1057 13. Scanning electron microscope photographs of specimens isolated from Vie River st. 10
1058 (46.70°N, 1.94°W, France). All scale bars = 10 μ m.

1059
1060 Plate 5. *Trinovantedinium applanatum* type A and B occurring in recent sediments. 1–2, 5–7.
1061 Different views of single specimen from Type A from station 1 (32.93°N, 129.86°E, 11.1 m
1062 water depth, Omura Bay, Japan). 3. Type A from Red Sea (va01-200P, 0-5 cm depth, 16.67°N,
1063 41.32°E, , 84 m water depth). 4. Specimen from 1–2 cm core depth from core CIRCE03AR 25P
1064 (15.30°N, 83.39°E, 3145m water depth, Bay of Bengal). 8–9. Type B from sample 11B
1065 (35.87°W, 64.11°N, 1318 m water depth, offshore Greenland, Boessenkool et al. 2001). 10. Type
1066 B from sample 1B (60.02°N, 11.76°W, water depth unknown, offshore Greenland, Boessenkool
1067 et al. 2001). All scale bars = 10 μ m.

1068
1069 Plate 6. 1–11. *Trinovantedinium variabile*. 1–6. Specimen from Saanich inlet (UVic 13-303-1,
1070 48.59°N, 123.50°W, water depth 226 m). 7–9. Other specimen from sediment-trap from Saanich
1071 Inlet (UVic 09-183, slide 1, 48.65°N, 123.48°W, water depth 96 m), previously studied by Price
1072 and Pospelova (2011). 10–11. Scanning electron microscope photographs of two specimens from
1073 sample Exp37A from Saanich Inlet (48.55°N, 123.53W, water depth 215 m). Figures 12–14.
1074 *Selenopemphix undulata* from Brentwood Bay, BC, Canada, sequenced through single-cell PCR.
1075 All scale bars = 10 μ m.

1
2
3
4
5
6
7
8
9
10
11
12
13
14
15
16
17
18
19
20
21
22
23
24
25
26
27
28
29
30
31
32
33
34
35
36
37
38
39
40
41
42
43
44
45
46
47
48
49
50
51
52
53
54
55
56
57
58
59
60



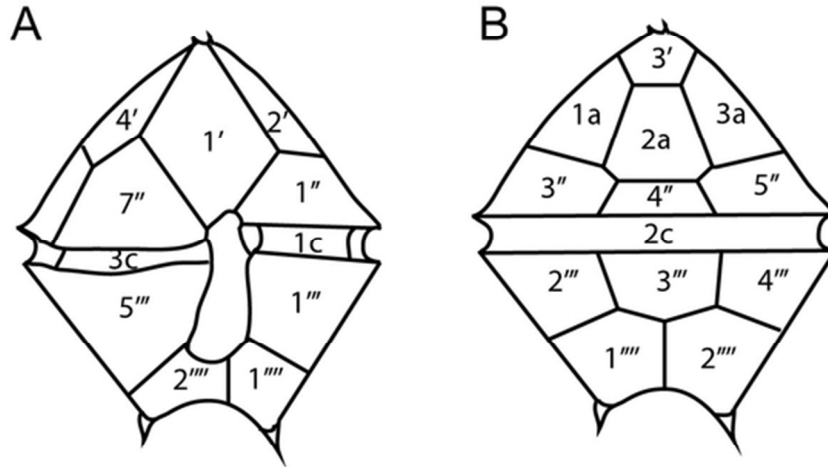
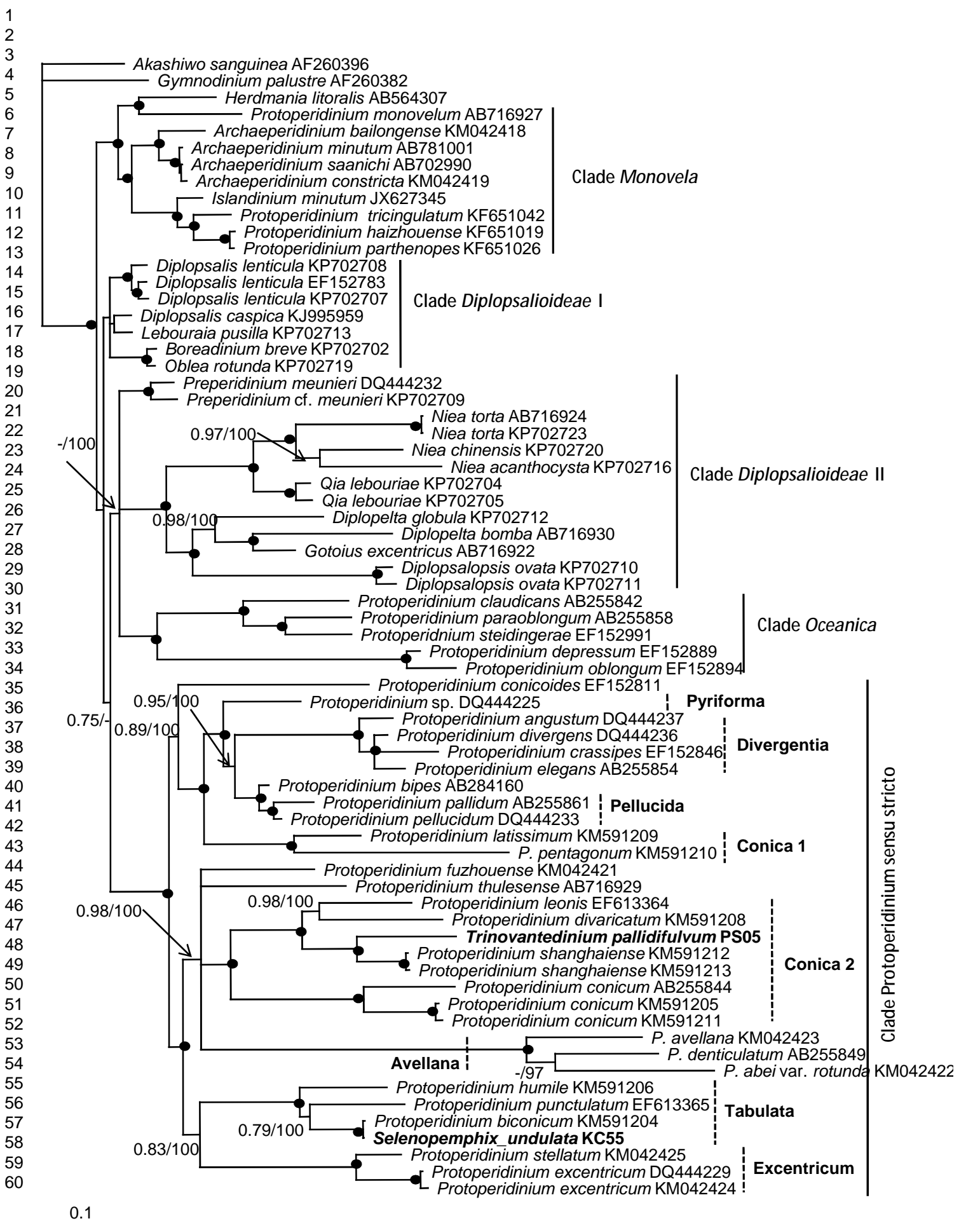
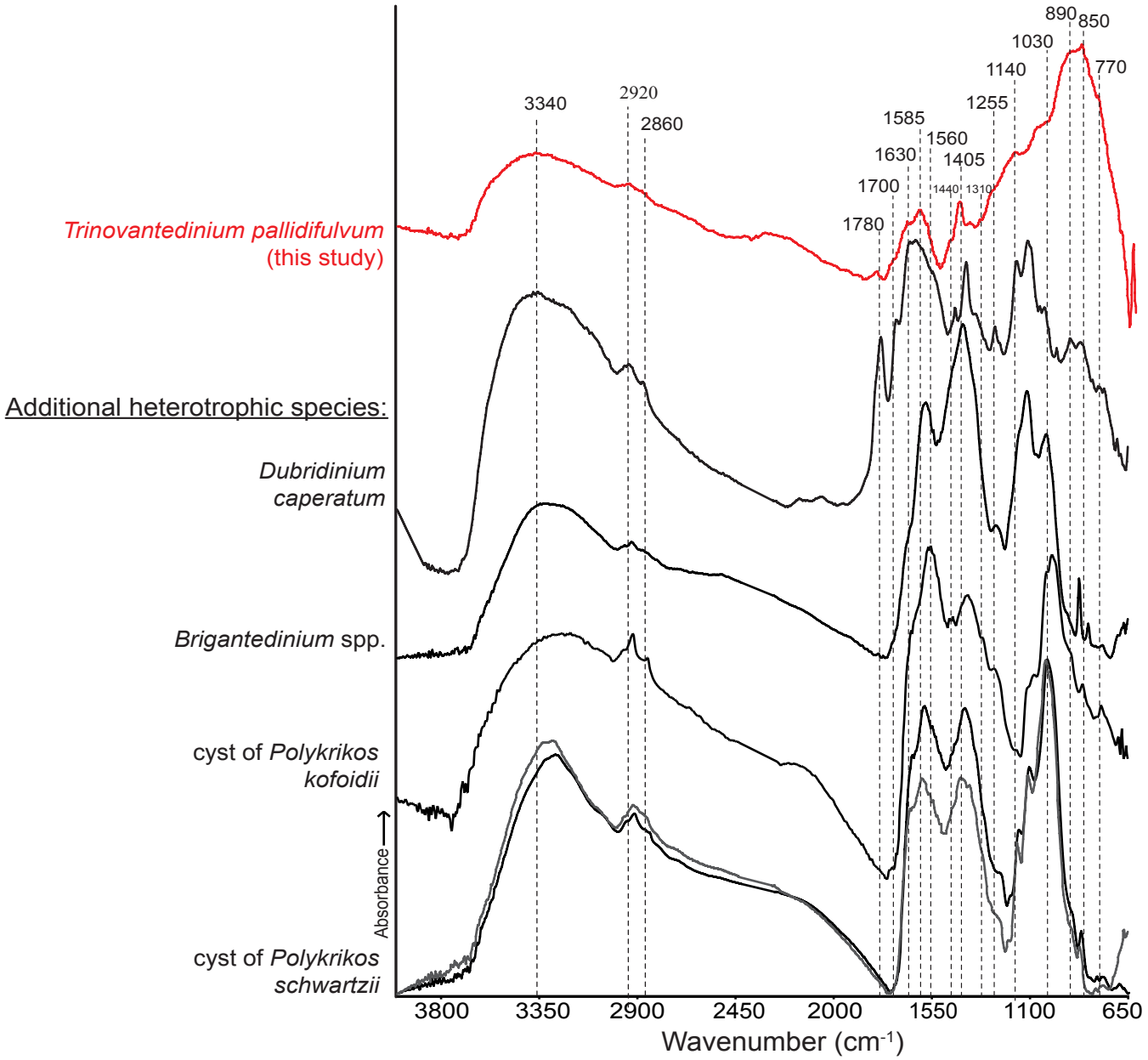
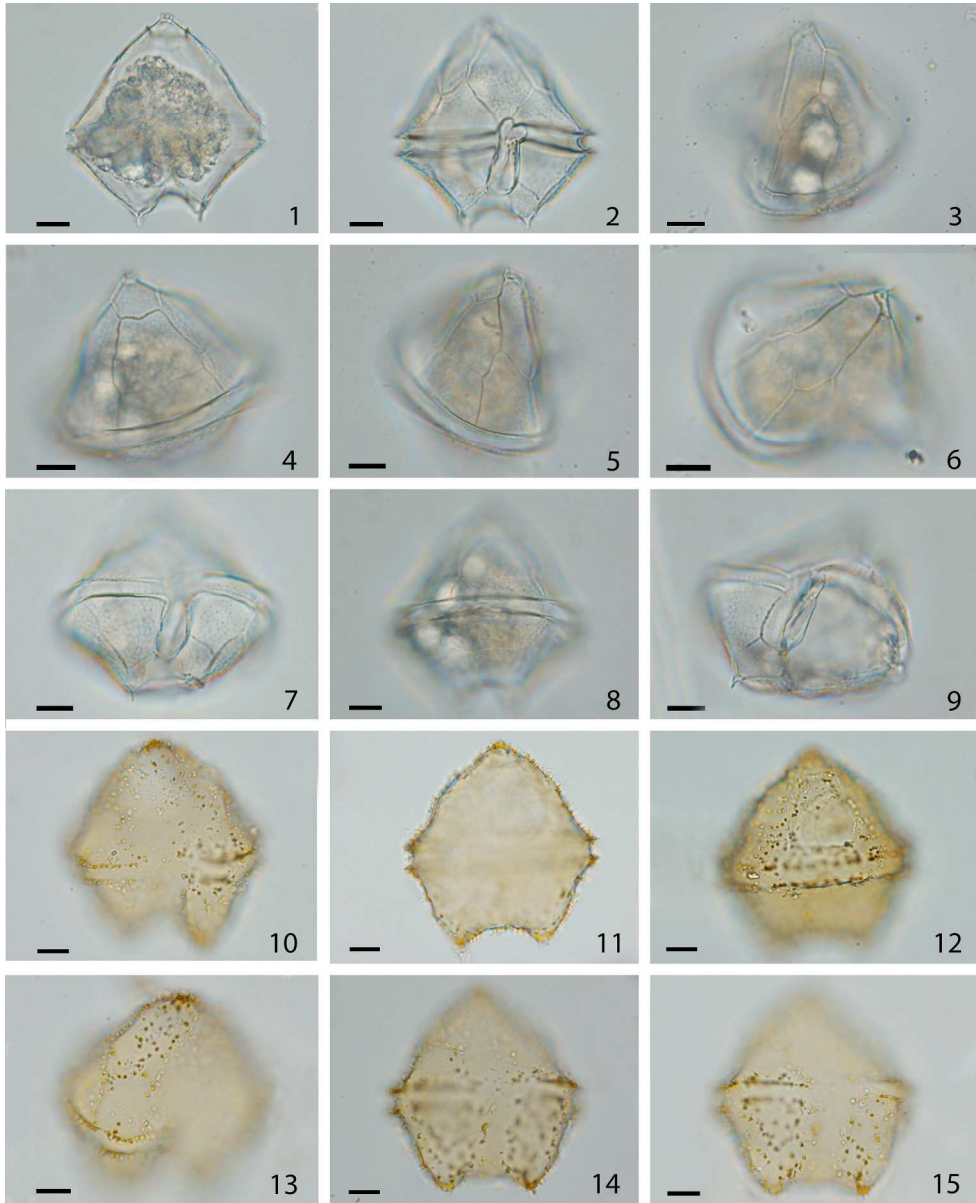


Figure 2. Drawings of *Protoperidinium lousianensis* n. sp. A). Ventral view. B). Dorsal view.
55x33mm (300 x 300 DPI)



1
2
3
4
5
6
7
8
9
10
11
12
13
14
15
16
17
18
19
20
21
22
23
24
25
26
27
28
29
30
31
32
33
34
35
36
37
38
39
40
41
42
43
44
45
46
47
48
49
50
51
52
53
54
55
56
57
58
59
60

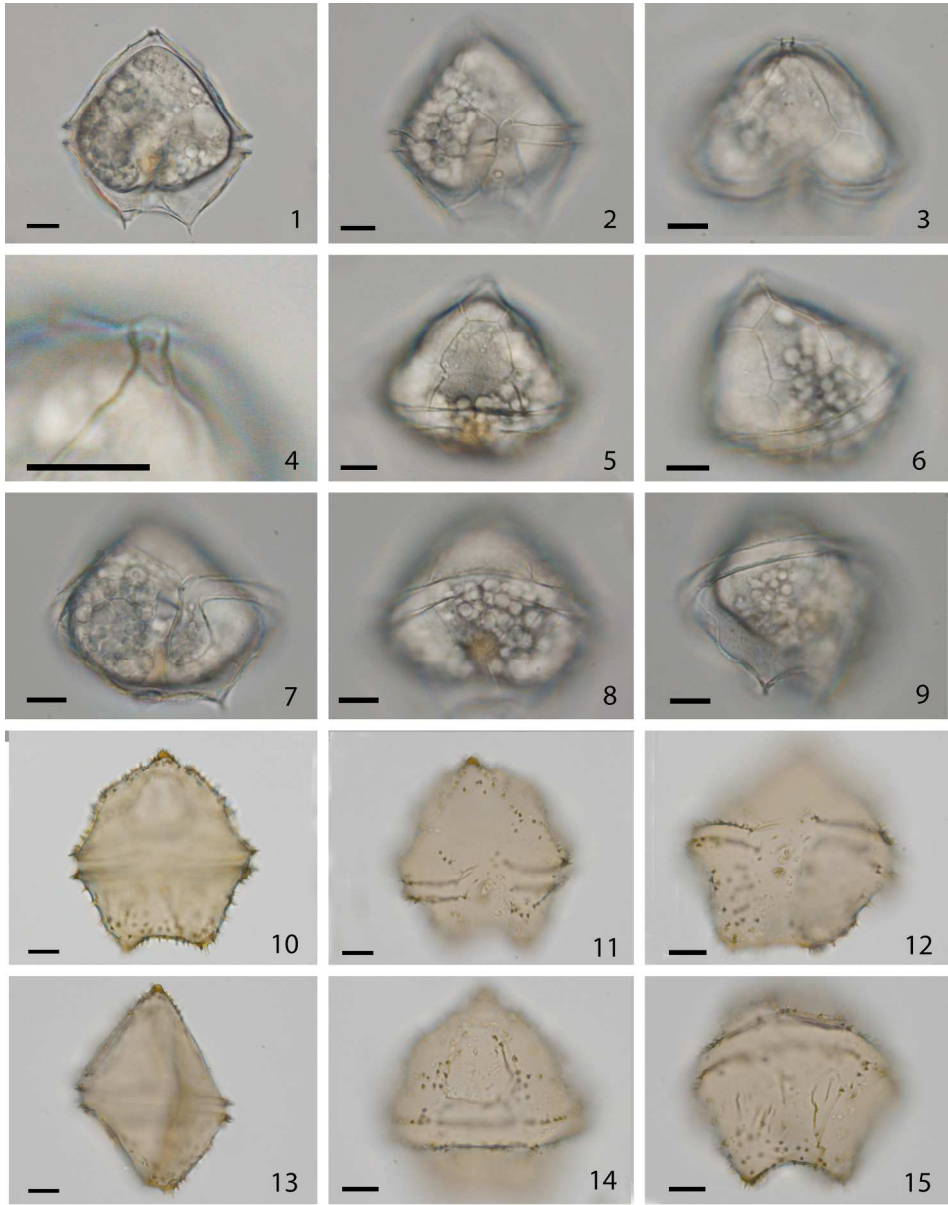




209x258mm (300 x 300 DPI)

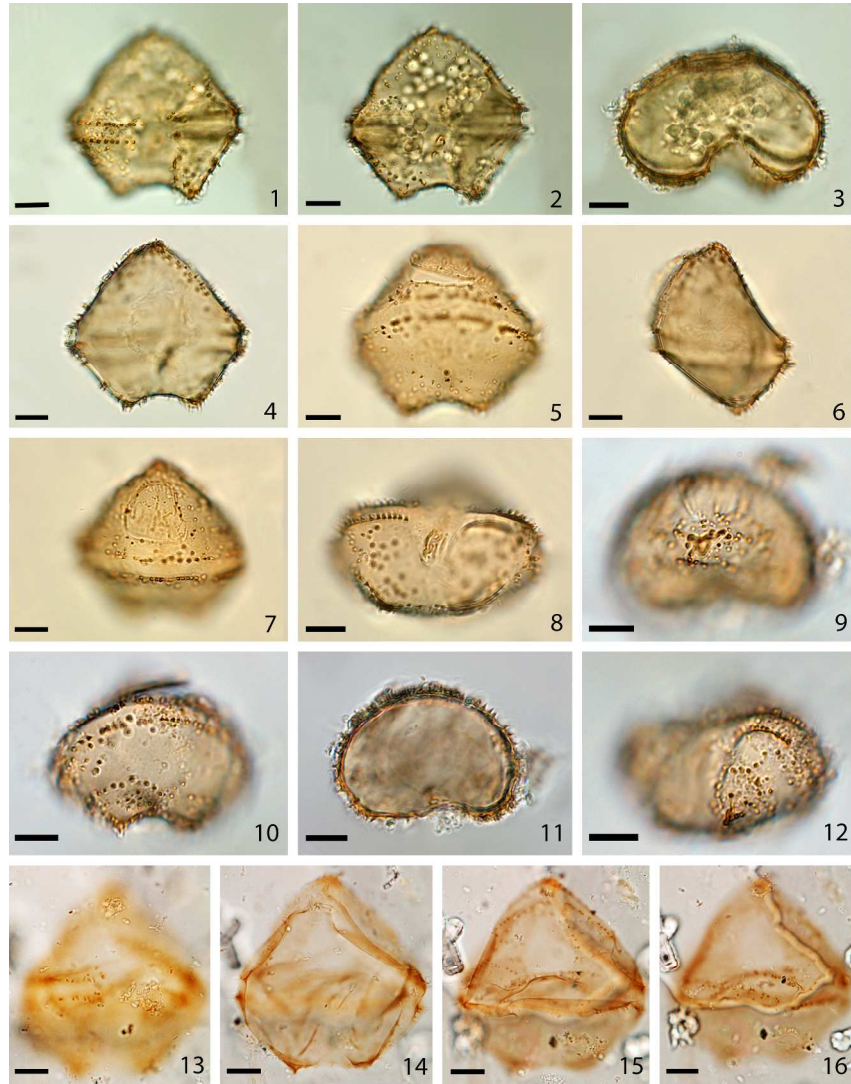
1
2
3
4
5
6
7
8
9
10
11
12
13
14
15
16
17
18
19
20
21
22
23
24
25
26
27
28
29
30
31
32
33
34
35
36
37
38
39
40
41
42
43
44
45
46
47
48
49
50
51
52
53
54
55
56
57
58
59
60

1
2
3
4
5
6
7
8
9
10
11
12
13
14
15
16
17
18
19
20
21
22
23
24
25
26
27
28
29
30
31
32
33
34
35
36
37
38
39
40
41
42
43
44
45
46
47
48
49
50
51
52
53
54
55
56
57
58
59
60



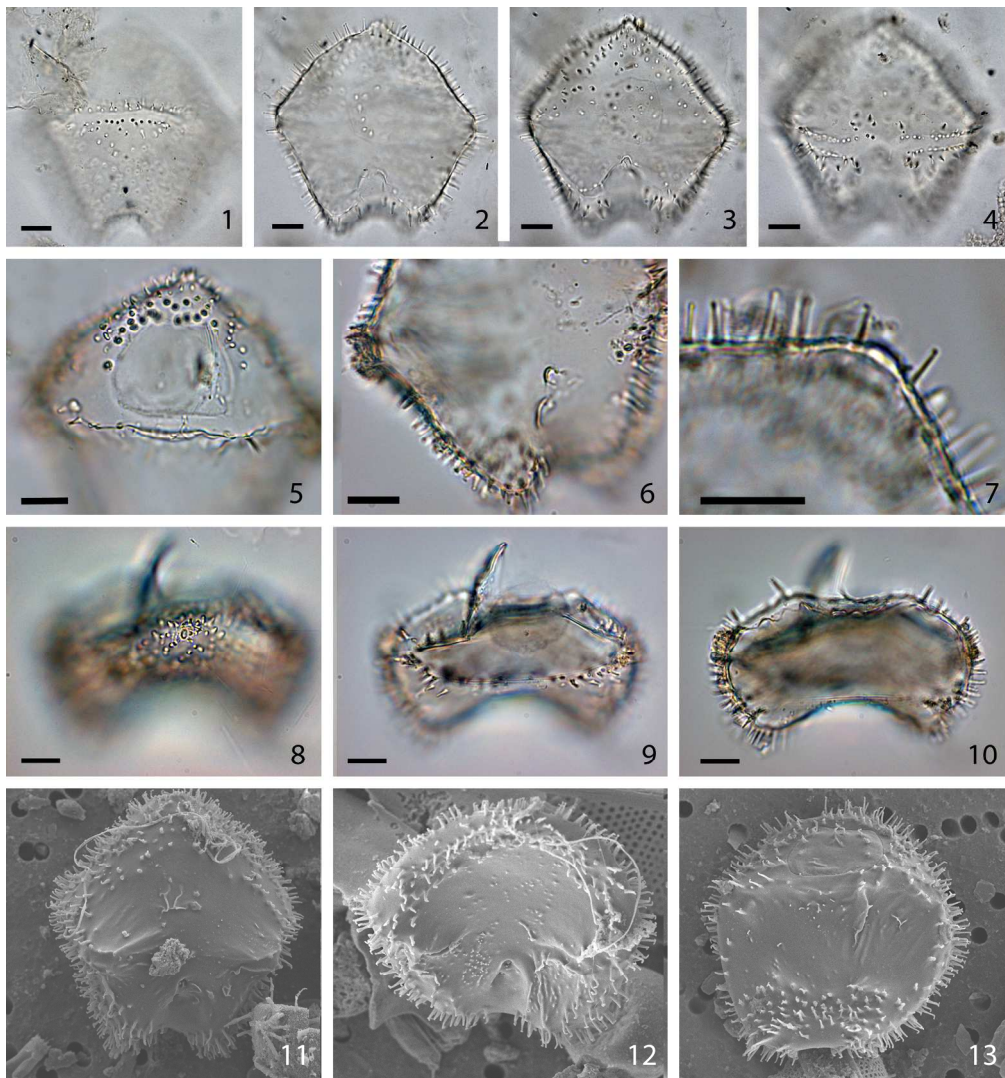
209x267mm (300 x 300 DPI)

1
2
3
4
5
6
7
8
9
10
11
12
13
14
15
16
17
18
19
20
21
22
23
24
25
26
27
28
29
30
31
32
33
34
35
36
37
38
39
40
41
42
43
44
45
46
47
48
49
50
51
52
53
54
55
56
57
58
59
60



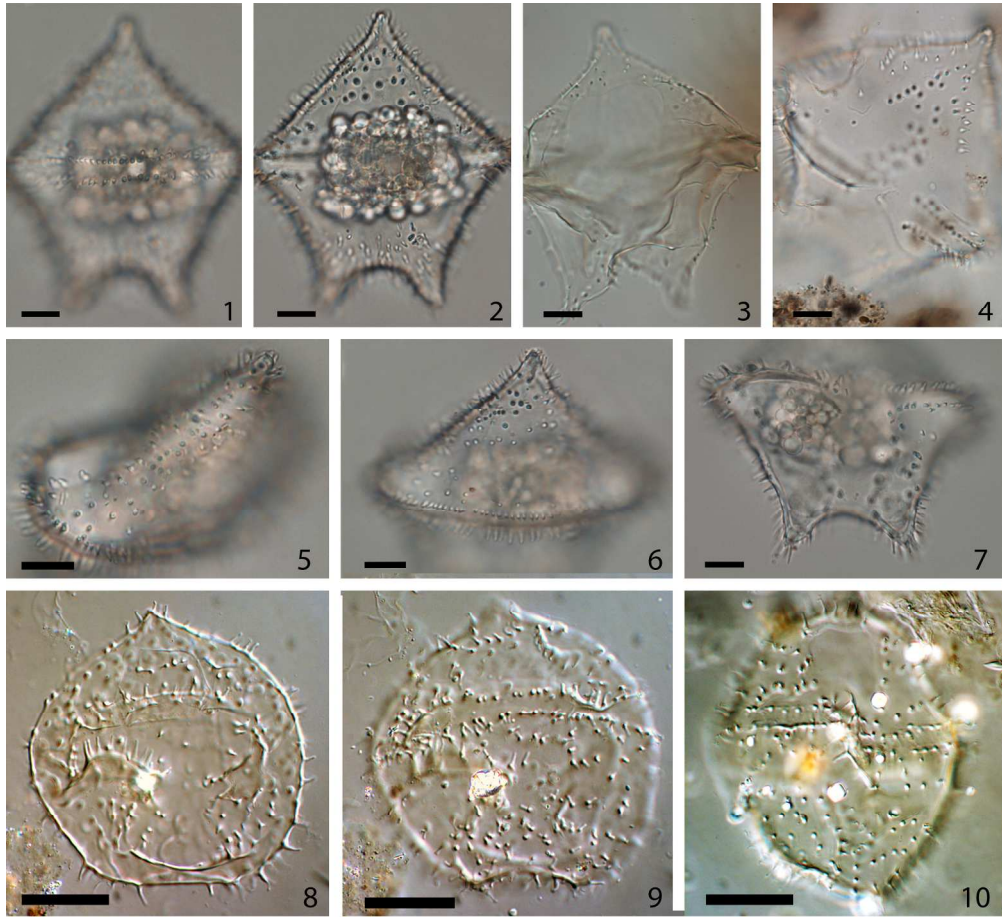
209x297mm (300 x 300 DPI)

1
2
3
4
5
6
7
8
9
10
11
12
13
14
15
16
17
18
19
20
21
22
23
24
25
26
27
28
29
30
31
32
33
34
35
36
37
38
39
40
41
42
43
44
45
46
47
48
49
50
51
52
53
54
55
56
57
58
59
60



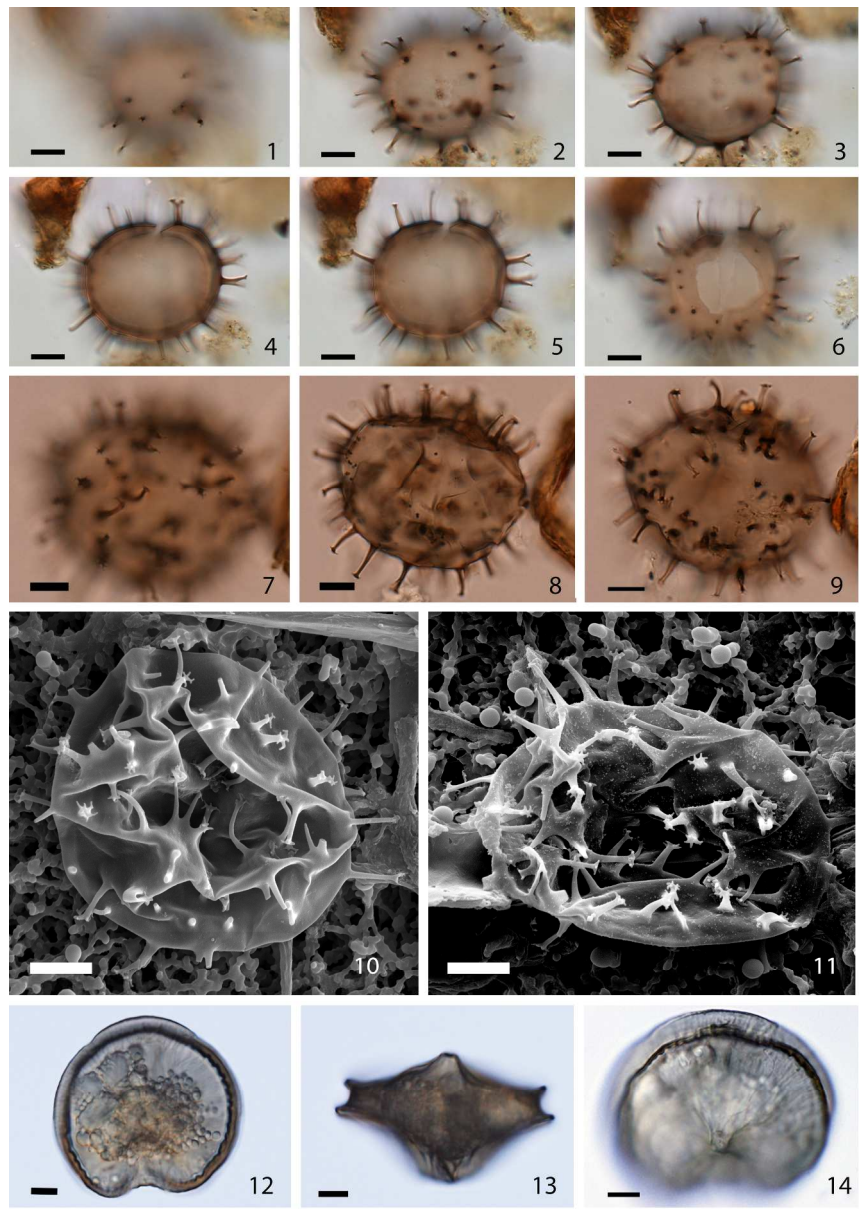
209x225mm (300 x 300 DPI)

1
2
3
4
5
6
7
8
9
10
11
12
13
14
15
16
17
18
19
20
21
22
23
24
25
26
27
28
29
30
31
32
33
34
35
36
37
38
39
40
41
42
43
44
45
46
47
48
49
50
51
52
53
54
55
56
57
58
59
60



209x191mm (300 x 300 DPI)

1
2
3
4
5
6
7
8
9
10
11
12
13
14
15
16
17
18
19
20
21
22
23
24
25
26
27
28
29
30
31
32
33
34
35
36
37
38
39
40
41
42
43
44
45
46
47
48
49
50
51
52
53
54
55
56
57
58
59
60



209x297mm (300 x 300 DPI)